ACKNOWLEDGEMENTS

Ever since the first bachelor years here in Hasselt University, I was intrigued by the field of stem cell research. Therefore, I was lucky when I was selected to do my bachelor training in this exciting research field. I was even more thrilled when I got the opportunity once again, to perform research at the Morphology department of Hasselt University. With this thesis, I consequently complete six beautiful years of being a student in Biomedical Sciences, something which would have never occurred without the support of several people.

First of all, I would like to thank my principal supervisor Prof. dr. Tom Struys for giving me the opportunity to participate and contribute to this interesting internship in his research group. I strongly believe in the need of cancer research and this project gave me the occasion to develop my research skills in a project I loved to do.

Special thanks go to my daily supervisor dr. Esther Wolfs. She introduced me to cloning and cellular transfection, or as we like to call it 'Cloning madness', which was a new and challenging experience for me. Her patience and infinite good-temperament always gave the day a positive twist. I would also like to thank her for her confidence in me and the nice talks we had once in a while. She prepared me for my future in research by letting me work individually and letting me plan my own experiments. Therefore, I am really grateful of being her senior student.

Furthermore, I would like to thank the other members of the morphology team for the constructive advice when needed and the amusing atmosphere. Also a word of appreciation goes to Jeanine Santermans and Marc Jans for their experience and help with immunohistochemical stainings and the electron microscope.

Of course, I am thankful for completing my internship with my fellow students. Afternoons could be quite noisy and hectic, yet amusing. I wish you all the best of luck in the future!

Finally, I would like to thank my friends, boyfriend and family for their support and advice throughout my thesis and whole education.

TABLE OF CONTENTS

LIST OF ABBREVIATIONS I
ABSTRACT III
SAMENVATTING V

1. INTRODUCTION 1
1.1 Clinical manifestation of oral squamous cell carcinomas 1
1.2 Current treatment strategies for oral squamous cell carcinomas 1
1.3 Gene therapy and suicide gene therapy 2
1.3.1 The principle of the Herpes Simplex Virus thymidine kinase/Ganciclovir system ... 2
1.4 Viral vector-mediated suicide gene therapy 3
1.4.1 Lentiviral vectors 4
1.5 Stem cell-mediated suicide gene therapy 4
1.5.1 The bystander effect 4
1.5.2 Stem cells in suicide gene therapy 5
1.5.3 human dental pulp stem cells in suicide gene therapy 6
1.6 The 4-nitroquinoline-1-oxide animal model 6
1.7 Molecular imaging 7
1.8 Hypothesis and experimental setup 7
1.8.1 Validation of suicide gene therapy *in vitro* 7
1.8.2 Optimization of the 4-nitroquinoline-1-oxide rat model 8
1.8.3 Scientific and societal relevance 8
2. MATERIALS AND METHODS 9
2.1 Isolation and culture of human dental pulp stem cells 9
2.2 Cell culture of squamous carcinoma cells 9
2.3 Immunocytochemistry 9
2.4 Transmission electron microscopy 10
2.5 Expression vector construction 10
2.5.1 Insertion of multiple cloning sites 11
2.5.2 Insertion of the suicide gene 12
2.5.3 Translocation towards an human elongation factor 1α promotor regulated plasmid 12
2.5.4 Transformation of NEB 5-alpha Competent E. Coli 12
2.5.5 DNA extraction and restriction analysis 13
2.5.6 DNA sequencing 13
2.6 human dental pulp stem cell transfection and luminescence assay 13
2.7 Optimization of the 4-nitroquinoline-1-oxide rat model 14
2.7.1 Treatment protocol 14
2.7.2 Perfusion and tissue isolation 14
2.7.3 Masson's Trichrome staining 14
2.7.4 Immunohistochemistry 15

3. RESULTS 17
3.1 human dental pulp stem cells and tumor cells form gap junctions 17
3.1.1 Connexin 43 expression is present in tumor and human dental pulp stem cell co-cultures 17
3.1.2 Cellular interactions contain gap junctions in tumor and human dental pulp stem cell co-cultures 19
3.2 Restriction analysis confirmed the generation of the expression vector 20
3.2.1 Insertion of the multiple cloning sites 20
3.2.2 Insertion of the suicide gene into the expression plasmid 21
3.2.3 Translocation towards an human elongation factor 1α promotor regulated plasmid 22
3.3 The designed expression plasmid was functional 23
3.4 Chronic 4-nitroquinoline-1-oxide administration resulted in oral dysplasia in rats 24
4. DISCUSSION 27
4.1 Morphological and ultrastructural analysis of co-cultures 27
4.2 Expression vector design 28
4.3 The 4-nitroquinoline-1-oxide rat model..... 29
4.4 Overall considerations and future perspectives 30
5. CONCLUSION 33
REFERENCES 35
SUPPLEMENTARY INFORMATION 39

LIST OF ABBREVIATIONS

α-MEM	Minimal Essential Medium, alpha modification
ATP	Adenosine triphosphate
BLI	Bioluminescence imaging
BM-MSC	Bone marrow mesenchymal stem cells
BSA	Bovine serum albumin
CMV	Cytomegalovirus
CRISPR	Cluster of regularly interspace short palindromic repeats
DAB	3,3'-Diaminobenzidine
DMEM/F12	Dulbecco's modified Eagle's medium Nutrient mixture F-12 HAM
DNA	Deoxyribonucleic acid
EF1α	Human elongation factor 1-alpha promotor
EGF	Epidermal growth factor
EGFR	Epidermal growth factor receptor
FBS	Fetal bovine serum
Fluc	Firefly luciferase
GCV	Ganciclovir
GDEPT	Gene-directed enzyme prodrug therapy
hDPSC	Human dental pulp stem cells
HGF	Hepatocyte growth factor
HIV	Human immunodeficiency virus
hNIS	Human sodium iodide symporter
HPV	Human papillomavirus
HSV-tk/TK	Herpes Simplex Virus type 1 thymidine kinase gene/protein
IRES	Internal ribosome entry site
Kb	kilo bases
LV	Lentiviral vector
MAGEA3	Melanoma-associated antigen 3
MCS	Multiple cloning site
MHC	Major histocompatibility complex
MRI	Magnetic resonance imaging
OSCC	Oral squamous cell carcinoma
PBS	Phosphate buffered saline
PCR	Polymerase chain reaction
PFA	Paraformaldehyde
ROS	Reactive oxygen species
RT	Room temperature
SDF-1	Stromal cell-derived factor 1
TALEN	Transcription activator-like effector nucleases
TEM	Transmission electron microscopy
T2A	2A peptide
UM-SCC-14C	Human mouth squamous cell carcinoma cell line 14C
ZFN	Zinc-finger nucleases
4NQO	4-Nitroquinoline-1-oxide

ABSTRACT

Introduction: Annually, over 300,000 people are diagnosed with oral squamous cell carcinoma (OSCC). Current treatment strategies of OSCC are associated with severe discomfort. Therefore, new treatment options need to be explored.
Suicide gene therapy involves the expression of a gene encoding a prodrug-activating enzyme and the subsequent administration of its nontoxic prodrug which, when activated, forms cytotoxic metabolites. Frequently, suicide gene therapy is accomplished by the viral vector-mediated transduction of tumor cells. However, the use of viral vectors implies several safety concerns and drawbacks.
In this thesis, the promising role of human dental pulp stem cells (hDPSC) as suicide gene carriers to treat OSCC is evaluated under the hypothesis that for suicide gene therapy, hDPSC are a valid gene carrier.

Materials and Methods: hDPSC were extracted from wisdom teeth and cultured in the presence of human oral squamous cell carcinoma cells. Cellular interaction was determined using immunocytochemistry for connexin 43 and transmission electron microscopy (TEM). Furthermore, an expression plasmid was generated containing the suicide gene and firefly luciferase. Gene functionality was evaluated through luciferin incubation after hDPSC transfection. Additionally, a representative OSCC rat model was optimized and assessed for future *in vivo* trials. Carcinogenesis was valued by means of Masson's Trichrome and immunohistochemistry against different proteins.

Results and Discussion: Immunocytochemistry indicated connexin 43 expression in hDPSC and tumor cell co-cultures. Connexin 43 expression seemed to be polar and present on cells located in a cell-dense region. Ultrastructural analysis of co-cultures revealed membrane thickening and electron-dense areas in membranes of cell-cell contacts. Both results combined are a strong indicative for gap junction formation between hDPSC and tumor cells. However, to confirm this statement, immuno-gold labelling against a tumor marker in combination with TEM is recommended to distinguish the two cell types on a non-morphological basis. Moreover, an expression plasmid with the suicide gene and firefly luciferase was produced. hDPSC transfection indicated proper gene functionality by firefly luciferase activity for one clone. Carcinogen administration in rats resulted in tongue dysplasia characterized by a disturbed tongue morphology and the expression of several markers e.g. connexin 43 and the melanoma-associated antigen 3 (MAGEA3).

Conclusion: Our data implicates the use of hDPSC as an alternative gene delivery method in suicide gene therapy when compared with viral vector gene delivery. The key finding suggesting this matter is the formation of functional gap junctions. Gap junction formation between hDPSC and SCC has never been proven before and is essential for the transport of the activated prodrug from hDPSC towards tumor cells. The cytotoxic capacity of HSV-tk expressing hDPSC could not be evaluated thus far. Future research on tumor cell survival will elucidate the role of hDPSC in suicide gene therapy more accurately.

SAMENVATTING

Introductie: Ruim 300.000 mensen worden jaarlijks gediagnostiseerd met een oraal squameuze cel carcinoma (OSCC). De behandeling van OSCC wordt geassocieerd met ernstige ongemakken, hetgeen de vraag naar alternatieve therapieën doet stijgen. Eén mogelijk alternatief voor de behandeling van OSCC, is zelfmoordgentherapie. Zelfmoordgentherapie is gebaseerd op de expressie van een prodrug-activerend enzym dat een niet-toxisch prodrug kan omzetten naar een cytotoxisch metaboliet, hetgeen lethaal is voor de cel.
Over het algemeen wordt zelfmoordgentherapie bekomen door de transductie van tumorcellen zelf. Virale vectoren worden in deze context gebruikt voor zelfmoordgen overdracht, nagenoeg met vele neveneffecten. In deze thesis wordt de rol van humane dentale pulp stamcellen (hDPSC) als zelfmoordgendrager onderzocht voor de behandeling van OSCC, onder de hypothese dat hDPSC geschikte gendragers zijn voor zelfmoordgentherapie.

Materiaal en methoden: hDPSC werden geëxtraheerd uit wijsheidstanden en samen in kweek gebracht met humane OSCC kankercellen. Celinteractie tussen beide celtypen werd bepaald door middel van immunocytochemie en transmissie elektronen microscopie (TEM). Vervolgens werd een plasmide aangemaakt die het zelfmoordgen en het vuurvlieg luciferase bevatte. Genetische functionaliteit werd onderzocht door middel van luciferine-incubatie na hDPSC transfectie. Daarenboven werd ook een representatief OSCC rat model geoptimaliseerd voor toekomstige *in vivo* experimenten. Een Trichroom van Masson kleuring en immunohistochemie voor verschillende merkers werden hiervoor toegepast.

Resultaten en Discussie: Immunocytochemie op de co-culturen duidde op connexine 43 expressie van tumorcellen en hDPSC. Connexine 43 werd hierbij voornamelijk polair op het celoppervlak waargenomen van de cellen in cel-rijke gebieden. Ultrastructurele analyse toonde elektronen-dense membranaire gebieden aan op plaatsen van cel contact. Deze membraan-verdikkingen waren waarneembaar tussen hDPSC, tumorcellen en beide celtypen. Beide resultaten duidden op de aanwezigheid van gap junctions tussen tumorcellen en hDPSC. Om deze vaststelling te bevestigen wordt een immuno-goud kleuring tegen een tumor merker aangeraden.
Verder is een plasmide aangemaakt met het zelfmoordgen en het vuurvlieg luciferase. Transfectie van hDPSC bevestigde de productie van een functioneel construct na luciferine-incubatie.
Carcinogeen-toediening in ratten veroorzaakte tongdysplasie gekenmerkt door een verstoorde morfologie en de expressie van verschillende merkers als connexine 43 en het melanoma geassocieerde antigen 3 (MAGE3).

Conclusie: Onze data duidt op het gebruik van hDPSC als alternatief voor virale vectoren in zelfmoordgentherapie. Een sterk indicatief hiervoor is de vorming van gap junctions tussen tumorcellen en hDPSC, essentieel voor het transport van de actieve prodrug. Het testen van de cytotoxische capaciteit van de zelfmoordgen-expresserende hDPSC is tot nu toe nog niet gebeurd. Toekomstig onderzoek op overleving van de tumorcellen zal meer inzicht geven over de rol van hDPSC in zelfmoordgentherapie.

1. INTRODUCTION

Head and neck cancer is the sixth most common type of cancer worldwide. Over one third of this heterogeneous group of malignancies is attributed to oral squamous cell carcinomas (OSCC) present in the oral cavity and oropharynx (1, 2). Globally over 300,000 new patients are reported each year, of which approximately 60% are originated from developing countries (3, 4). Furthermore, the incidence and mortality of OSCC are still rising including in The Netherlands and other European countries (2, 5). This increase as well as the global distribution of OSCC is largely associated with the prevalence of the main risk factors of the malignancy; tobacco consumption, alcohol use, ultraviolet radiation and human papillomavirus (HPV) infections (4, 5).

1.1 Clinical manifestation of oral squamous cell carcinomas

OSCC itself often resembles a persistent ulcerated mass, nodule and/or an irregular red velvet patch. White or red mucosal colour changes known as leukoplakia and erythroplakia are often the first sign of OSCC development (Figure 1) (4, 5). Both are recognized as pre-existing potentially malignant disorders with a malignant transformation rate of nearly 20% for leukoplakias to nearly 90% for erythroplakias (5). Symptoms are often absent during these early disease stages and frequently arise when the tumor becomes invasive or grows extensively (4). In addition, the clinical manifestation of OSCC (e.g. dysphagia or difficulty in swallowing, weight loss, sore throat and hoarseness) rather mimics common benign conditions, making it hard to diagnose OSCC early (4, 5).

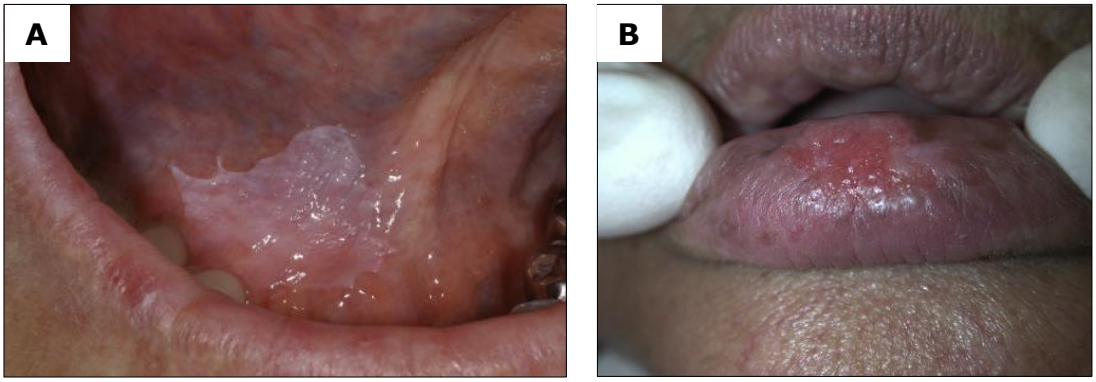

Figure 1: Demonstrative images of leukoplakia and erythroplakia in patients.
(A) The discrete white patch on the right floor of the mouth shows hyperkeratosis and is known as leukoplakia. **(B)** The long lasting red patch on the lower lip of this patient is recognized to be erythroplakia (Pictures adapted from (4)).

1.2 Current treatment strategies for oral squamous cell carcinomas

Depending on the disease stage, the patient physical well-being (e.g. age and comorbidities) and the location of the primary tumor, different treatment strategies can be applied. Current OSCC therapy consists of surgery, radiotherapy and chemotherapy or a combination of these (4, 5).

Despite favourable responses to OSCC treatment, the prognosis of OSCC remained unchanged over the past decades, with an average 5-year survival rate of 50% (1). Moreover, several negative consequences of OSCC therapy are observed. Surgical tumor resection for example is often accompanied by functional deficits, affecting speaking, eating, drinking, chewing and swallowing

abilities (5). Additionally, the esthetical changes following surgery have a great psychological impact. Complicated cosmetic reconstructions of deformities or treatment-related functional defects are therefore frequently necessary (6). Finally, complications of chemotherapy and radiotherapy such as oral or bone marrow toxicity, soft tissue necrosis, inflammation and infertility can arise. These acute and late toxicities are furthermore underreported and under-recognized, leading to an additional decrease of the patient's quality of life (7, 8). For these reasons, new, safer and tumor-specific OSCC treatments need to be developed. This to improve the patient's quality of life and survival rate, but also to reduce the observed complications.

1.3 Gene therapy and suicide gene therapy

Gene therapy became the focus of the development of new cancer therapies in which therapeutic genes are used to affect tumor growth. As such, several strategies for cancer gene therapy arose including the transfer of tumor suppressor genes and the inhibition of activated oncogenes by antisense oligonucleotides (9). However, this kind of gene therapy mainly targets one of the several genes responsible for the malignant transformation. In addition, not all tumor cells have the same genetic background as tumors are highly heterogeneous. Therefore, the application of gene therapy that can operate independently from the genetic background of the tumor cells is recommended (10, 11). Suicide gene therapy, also called gene-directed enzyme prodrug therapy (GDEPT) is one such therapy. The application of suicide gene therapy, relies on the local delivery of a selective prodrug-activating enzyme, a so-called 'suicide gene'. To mediate an effect, a nontoxic prodrug will be administrated, which forms cytotoxic metabolites when activated (8, 12).

1.3.1 The principle of the Herpes Simplex Virus thymidine kinase/Ganciclovir system

The most extensively studied and pioneering suicide gene is the Herpes Simplex Virus type 1 thymidine kinase (HSV-tk) gene combined with its prodrug ganciclovir (GCV), which was first reported to be a possible cancer treatment by Moolten et al. in 1986 (11, 13). As some other suicide genes, HSV-tk encodes for a nucleotide-metabolizing enzyme (8). Specifically, HSV-TK potentiates the phosphorylation of thymidine, deoxythymidylate and guanosine analogues (8). One such non-toxic guanosine analogue is GCV, known in the clinic for the treatment of cytomegalovirus (CMV) infections (8).

In suicide gene therapy, the phosphorylation of GCV results in its cellular entrapment and cell death by a process involving several steps. First, GCV is phosphorylated by HSV-TK to GCV-monophosphate. Next, monophosphorylated GCV is recognized and phosphorylated by endogenous enzymes (guanylate kinase and nucleoside diphosphokinase) creating GCV-triphosphate. The resulting cytotoxic guanine nucleoside analogue incorporates into the deoxyribonucleic acid (DNA) during mitosis, causing DNA chain termination and the eventual observed lethal cellular events including the induction of mitochondrial damage (Figure 2) (8, 10, 14, 15).

Over time, different variants of HSV-tk were developed by random mutagenesis to increase the activity towards GCV and reduce possible side effects of the prodrug (8). One such HSV-tk gene variant is HSV1-SR39tk who contains a point mutation in serine 39, resulting in a 294-fold reduction in the required prodrug dose relative to the wild type HSV-tk gene. As a result, the affinity of HSV-

SR39TK towards GCV became a 1000-fold higher when compared with endogenous thymidine kinases, leading to cytotoxic effects local to HSV-tk expressing cells (8, 10).

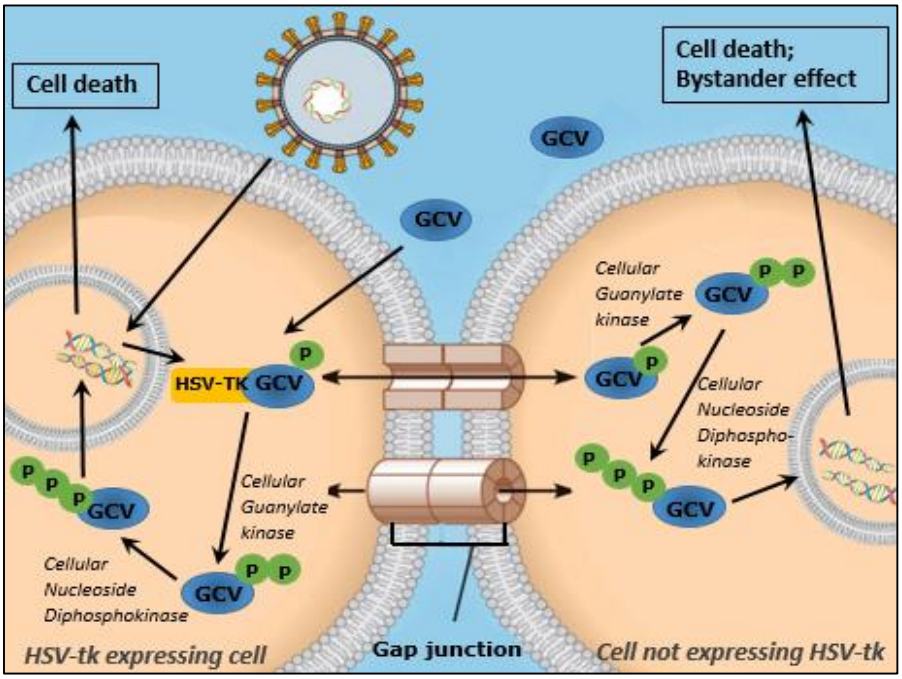

Figure 2: **The principle of suicide gene therapy and the local bystander effect.**
The administrated non-toxic prodrug ganciclovir (GCV) is converted to GCV-triphosphate (GCV-PPP) by the Herpes Simplex Virus Thymidine Kinase (HSV-TK) and endogenous kinases (Guanylate kinase and Nucleoside Diphosphokinase) in a HSV-tk expressing cell. During cell replication, triphosphorylated GCV competes with deoxyguanosine triphosphate for DNA incorporation. The resulting incorporation of GCV-PPP into the DNA leads to DNA chain termination and cell death of the HSV-tk expressing cell. Moreover, phosphorylated GCV can diffuse from the HSV-tk expressing cell towards other cells not expressing HSV-tk, this through the formation of gap junctions. Consequently, after the conversion of the phosphorylated GCV by the endogenous kinases, cytotoxic events are initiated there as well, this phenomenon is called 'the bystander effect' (8, 10, 14, 15).

1.4 Viral vector-mediated suicide gene therapy

To achieve local HSV-tk expression in suicide gene therapy, a functional gene delivery system needs to be implemented. The most abundantly applied delivery system is the implementation of viral vectors to directly target the tumor cells (11). Viral vectors are viral-derived particles still able to insert their genetic material into the host cell, yet are unable to replicate or infect cells. The single occurring gene transfer event used for gene delivery is called *transduction*. In viral vector-mediated suicide gene delivery, these viral vectors contain the suicide gene for the direct transduction of tumor cells.

Several promising clinical trials for glioma treatment among others with the HSV-tk suicide gene were obtained, most of them as a result of viral vector gene delivery (11). However, despite the relatively high transduction rate of viral vectors, safety concerns with the use of viral vectors for gene delivery dampened the enthusiasm for their wide-spread use. The direct injection of viral vectors or viral vector-producing cells might elicit damaging immunological reactions by triggering the immune system. In addition, viral vectors are not able to distinguish normal cells from tumor cells and have a limited diffusion capacity, making precise injection of the viral vectors into the tumor a necessity.

Furthermore, insertion of the viral genome into the host DNA occurs at random and on occasion multiple times, with the possibility to elicit insertional mutagenesis (9, 11). As a result, other delivery systems for suicide gene therapy were evaluated, including stem cell-mediated suicide gene therapy in which the stem cells stably express the suicide gene.

1.4.1 Lentiviral vectors

Viral vectors still can be utilized in order to achieve stable suicide gene expression in stem cells. One type of viral vector exploited to transduce stem cells for suicide gene therapy is the lentiviral vector (LV), a complex retroviral vector containing two single RNA strands. Lentiviral vectors are derived from the human immunodeficiency virus (HIV) and therefore evoke a relatively low immune response. Stable and long-term expression of the transgene in transduced (stem) cells is accomplished due to the integration of the transgene into the host DNA. This integration can take place for large sequences or multiple genes as LVs have a large genome size (9.6 kilo bases/kb) and transduction occurs in high rates as they are able to infect dividing and non-dividing cells (16).
Viral vectors are modified to maximize their safe use. Viral genes involved in viral replication are eliminated, leaving only structural, transcriptional and enzymatic components needed for stable DNA integration encoded on a construct plasmid. Chances of infection with these 'second generation' viral vectors is therefore reduced (16).

1.5 Stem cell-mediated suicide gene therapy

Stem cells are primitive undifferentiated cells capable of self-renewal and differentiation into minimally one specialized cell type (17). Based on the differentiation capacity, stem cells can be divided into four major types; totipotent stem cells, pluripotent stem cells, multipotent stem cells and unipotent stem cells (17). Totipotent stem cells are produced in the early stages of the embryogenesis and give rise to all cell types of the embryo and extra-embryonal tissues. In contrast to totipotent stem cells, pluripotent stem cells cannot form an entire organism. These embryonal stem cells generate germ cells or cell types originating from the three germ layers; the mesoderm, ectoderm and endoderm. Multipotent stem cells, also known as adult stem cells, generally give rise to cell types of their germ layer of origin. And lastly, unipotent or progenitor stem cells can differentiate into one defined cell type and possess limited self-renewal capacity (17).

1.5.1 The bystander effect

Stem cell-mediated suicide gene therapy is founded on the bystander effect, an extension of the lethal effects occurring in the HSV-tk expressing cells towards neighbouring (tumor) cells not expressing HSV-tk (Figure 2) (8). Therefore, the occurrence of the bystander effect is crucial for stem cell-mediated suicide gene therapy, lying at the base of the effectiveness of this treatment. Different mechanisms for the bystander effect have been proposed, dividing the bystander effect into local and immune-mediated categories (8, 14).

In the first case, a local killing zone around the HSV-tk expressing cell is created through the transfer of toxic metabolites (8, 14). The formation of gap junctions with cells not expressing HSV-tk, the internalization of apoptotic vesicles containing the activated prodrug by non-HSV-tk expressing cells

and the diffusion of soluble potentially toxic metabolites into non-transduced cells all may potentiate the local bystander effect (8, 14, 15). In case of GCV, the local bystander effect is mainly mediated through the formation of gap junctions since the purine nucleoside cannot passively diffuse across cell membranes when phosphorylated (10, 14). Gap junctions are ring-shaped cell-to-cell contacts made out of connexins responsible for the diffusion of ions, nucleotides and other small molecules (<1kDalton) like metabolites between adjacent cells (8, 10). Therefore, the major function of gap junctions is the maintenance of homeostasis and cell communication between neighbouring cells. Since the formation of gap junctions in OSCC is increased, occurrence of the intratumoral local bystander effect is highly likely (18).

Besides the local bystander effect, cytotoxic events may also occur out of the proximity of the suicide gene expressing cells, an immune response is lying at the base of the process. This immune-mediated bystander effect is the result of local inflammation directed towards the dying tumor cells and is called 'the distant bystander effect' (8, 14). An additional beneficial effect of the distant bystander effect is the reduction of tumor recurrence due to the production of memory cells directed against the tumor (14).

As a consequence of the complexity of suicide gene therapy, several factors determine its overall efficiency and outcome. First, the catalytic activity of the enzymes involved in the conversion of GCV to its cytotoxic form (8). Second, the growth rate of the tumor cells and time of prodrug administration since activated GCV is cytotoxic specifically in actively dividing cells (14, 19). Third, the extent of the bystander effect. Finally, the efficiency of the gene delivery system used; the more the therapeutic gene is locally expressed, the better (20).

1.5.2 Stem cells in suicide gene therapy

Several types of stem cells have already been evaluated for the stem cell-based delivery of suicide genes (21-23). In particular, the adult multipotent stem cells like adipose and bone marrow mesenchymal stem cells (BM-MSC) are used the most frequent (15). These MSC are hypoimmunogenic and can be easily isolated without ethical concerns in contrast to embryonic stem cells (15). In addition, like neural stem cells, it is shown that MSC display tropism directed against inflammatory mediators found at sites of injury but also at sites of tumor development (e.g. Stromal cell-derived factor 1 (SDF-1), epidermal growth factor (EGF) and hepatocyte growth factor (HGF)) (15, 24). Local engraftment of MSC into the stroma after tumor homing is acknowledged too, making these stem cells a potential vehicle for targeted gene therapy (24). An essential finding confirming this statement is the formation of gap junctions between the MSC and tumor cells. The transfer of phosphorylated GCV for that matter can arise, eventually resulting in tumor cell death (25).

As such, stem cell-mediated suicide gene therapy is grounded on the tumorotropic properties of stem cells. Tumor growth is affected through the bystander effect once the HSV-tk expressing stem cells are located at the tumor site and form gap junctions with the malignant cells. This gap junction formation is vital to propagate the passage of phosphorylated-GCV and its cytotoxic effects towards the tumor cells. Consequently, the use of stem cells as a gene carrier brings several advantages when compared with viral vectors, as migration towards tumor cells can arise and immune responses

remain limited. Moreover, the suicide gene expression of the stem cells leads to the implementation of a safety-switch, diminishing the risk of tumor formation by the injected stem cells (26).

1.5.3 human dental pulp stem cells in suicide gene therapy

Besides the use of adipose and bone marrow MSC in suicide gene therapy, the possible role of other MSC has to be explored in order to potentially improve suicide gene therapy even more.

Over the past decade, more MSC-like populations have been identified, including in different dental tissues such as the periodontal ligament, the apical papilla and the dental pulp (27-30). From the latter, stem cells were first isolated in 2000 by Gronthos et al. and given the name of human dental pulp stem cells (hDPSC) (31). These adult stem cells are considered to be ecto-mesenchymal due to the interaction with the neural crest during tooth development (32).

Nonetheless, hDPSC have very similar characteristics with BM-MSC such as adherence to a plastic surface, a fibroblast-like morphology and the ability to form colonies *in vitro* (31). And, like BM-MSC, these stem cells are capable to differentiate into cells of the mesodermal lineage e.g. chondrocytes, adipocytes and osteoblasts (32). The most important feature of hDPSC similar with other MSC is their hypoimmunogenic and immunoregulatory character based on major histocompatibility complex (MHC) and Fas ligand expression among others (33, 34).

Nevertheless, several advantages of hDPSC over BM-MSC have been reported, indicating that hDPSC are a new promising alternative stem cell source.

The large scientific interest in hDPSC knows several reasons, including the fact that these stem cells can be easily isolated from pulp tissue of discarded wisdom teeth. Extraction of hDPSC is therefore less invasive and easier when compared to the extraction of BM-MSC (35). The cell gain after *in vitro* expansion and cell derivation differs between the two cell types as well. hDPSC isolation out of dental pulp provides a higher cell amount and their proliferation potential is higher than that of BM-MSC, making the use of hDPSC more attractable (35).

Furthermore, hDPSC retain their stem cell properties after cryopreservation, offering the opportunity to create a stem cell bank which yields a great advantage for cell therapies (36). Based on these characteristics, hDPSC can be an ideal stem cell population for future suicide gene therapy. Still, there is no record of the utilization of hDPSC in suicide gene therapy yet.

1.6 The 4-nitroquinoline-1-oxide animal model

To evaluate the potency of suicide gene therapy in OSCC, investigation both *in vivo* and *in vitro* is desirable. Several animal models for OSCC are utilized including xenograft models which are widely used for the insurance and speed of tumor development (2). Another well-known animal model is the 4-nitroquinoline-1-oxide (4NQO) rat model first introduced by Wallenius et al. (37). This model is based on natural carcinogenesis and very similar (e.g. histologically and the expression of biomarkers) with human OSCC (2). Tumor development is obtained through the chronic administration of 4NQO, stimulating carcinogenesis in a similar way to its human counterparts (2).

4NQO is a synthetic carcinogen which induces a tumorigenic effect through the generation of reactive oxygen species (ROS). Oxidative stress in this process is the result of redox cycling of 4NQO, an enzymatic reduction of 4NQO followed by auto-oxidation in de presence of molecular oxygen (2).

Additionally, 4NQO molecules are capable to cause pyrimidine dimmer formation. These bulky DNA adducts are the result of DNA binding predominantly at guanine residues (2).

1.7 Molecular imaging

Besides the choice of a representative animal model, monitoring the applied therapy as well as the treatment response are vital for the optimization and clinical translation of stem cell-based therapies. This is also the case for suicide gene therapy. Molecular imaging can be implied in this context, enabling temporal analyzation of the stem cell-mediated treatment in a non-invasive matter.

One such non-invasive imaging technique is magnetic resonance imaging (MRI), an imaging modality founded on the magnetic potential of Hydrogen atoms (38). Depending on the constitution of the tissue, difference in imaging contrast is obtained, making the visualisation and distinction of soft tissues like a tumor possible (38).

Moreover, concerning stem cell-mediated suicide gene therapy, non-invasive spatial follow-up of the HSV-tk expressing stem cells offers more insight into the applied suicide gene therapy and its outcome. To visualize the HSV-tk expressing stem cells, bioluminescence imaging (BLI) can be applied (38). This imaging modality is based on the expression of the firefly luciferase (Fluc) reporter gene. Visualization of Fluc expressing cells occurs via the administration of D-luciferin, the substrate for Fluc, leading to the emission of visible light or photons. Consequently, in contrast to fluorescent imaging modalities, no external light excitation is needed, diminishing background noise and increasing the sensitivity (38). In addition, oxidation of D-luciferin is only possible under physiological conditions within living cells as adenosine triphosphate (ATP) and oxygen are needed. Consequently, the assessment of cell viability is possible too (38).

1.8 Hypothesis and experimental setup

Our research team questioned whether hDPSC are a suitable gene carrier for the mediation of suicide gene therapy, something which has never been done before. Preliminary data already indicated gap junction formation between hDPSC and an OSCC tumor cell line. Additionally, the tumor homing capacity of hDPSC was verified. Both aspects are favourable for the application of hDPSC in stem cell-mediated suicide gene therapy and led to the hypothesis that hDPSC are valuable mediators in suicide gene therapy.

1.8.1 Validation of suicide gene therapy *in vitro*

To evaluate the delivery capacity of hDPSC in suicide gene treatment for OSCC, gap junction formation was evaluated first. A co-culture with an OSCC cell line (human mouth squamous cell carcinoma cell line; UM-SCC-14C) was achieved for this purpose. Gap junction formation was analysed by immunocytochemistry and transmission electron microscopy (TEM). Next, hDPSC were transfected with the suicide gene using lipofectamine® 2000. The expression plasmid designed contained HSV-tk and Fluc. The latter to make future stem cell tracking with BLI possible.

1.8.2 Optimization of the 4-nitroqinoline-1-oxide rat model

Moreover, to validate hDPSC-mediated suicide gene therapy in the best circumstances as possible, the 4NQO rat model was optimized and evaluated to be a suitable model for OSCC. For this purpose, rats were administrated 4NQO manually on the tongue or in the drinking water and compared with one another. Two additional control groups were made to bypass the effect of stress and the vehicle propylene glycol. Validation and choice of the best rat model was based on *ex vivo* examinations with histology and immunohistochemistry after sacrificing the animals of the treatment cohorts at a monthly basis (Figure 3).

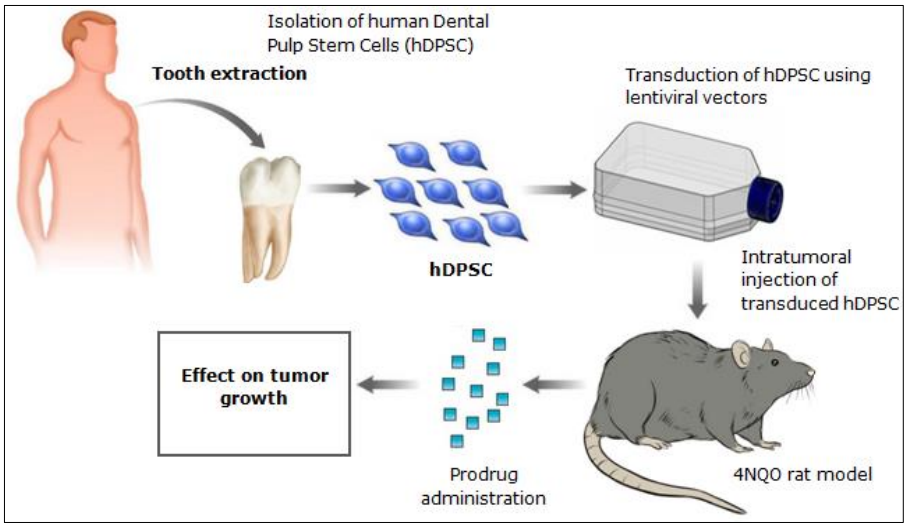

Figure 3: Schematic representation of the several steps and objectives of the current research.
First human dental pulp stem cells (hDPSC) are evaluated as a potential suicide gene mediator *in vitro*. Next, a 4-nitroquinoline-1-oxide (4NQO) rat model is optimized to later validate the potential of hDPSC-mediated suicide gene therapy *in vivo*.

1.8.3 Scientific and societal relevance

With this study, we hope to analyse the potency of hDPSC being a suicide gene carrier and their potential use in OSCC treatment in the most optimal manner. Getting a better understanding of this process may have an important impact on current suicide gene therapy research, optimizing the suicide gene delivery method with the stem cells that are most effective. Naturally, improvement of the current suicide gene therapy method can get us a step closer to more efficient OSCC treatment or cancer treatment in general, impacting thousands of lives a year.

2. MATERIALS AND METHODS

2.1 Isolation and culture of human dental pulp stem cells

The isolation of hDPSC was approved by the Medical Ethical Committee of Hasselt University (201424). Human dental pulp was collected from patients (15 to 25 years old) undergoing a routine extraction of third molars at Ziekenhuis Oost-Limburg (Genk, Belgium). These teeth were obtained with written informed consent from the patients themselves or their guardians in case of underage patients.

To acquire hDPSC, the wisdom teeth were mechanically fractured and the containing pulp tissue was carefully isolated using forceps. The tissue was placed in Minimal Essential Medium, alpha modification (α-MEM, Sigma-Aldrich, St-Louis, OM) supplemented with 10% fetal bovine serum (FBS, Gibco, NY, USA), 2 mM L-glutamine (Sigma-Aldrich), 100 U/mL penicillin (Sigma-Aldrich) and 100 µg/mL streptomycin (Sigma-Aldrich), also known as the standard medium of hDPSC. Afterwards, cells were harvested by performing the outgrowth method. Here fore, pulp tissue was fragmented into small pieces (1-2 mm^3) and cultured in 6-well plates (Greiner Bio-One, Alphen aan den Rijn, The Netherlands) in the culture medium previously mentioned, additionally supplemented with amphotericin B. Cell migration out of the explants was allowed for 14 days where after the explants were discarded from the culture dish. The subsequent cell population was harvested after reaching 80-90% confluency and serially passed by 0.05% trypsin/EDTA (ThermoFisher Scientific, NY, USA) dissociation for *in vitro* experiments. The hDPSC were maintained in their standard medium for cell culture, incubation took place at 37°C in the presence of 5% CO_2 and the medium was changed every 2-3 days. For the performed experiments, hDPSC from passage 3-14 were used.

2.2 Cell culture of squamous carcinoma cells

The utilized oral squamous carcinoma cells, UM-SCC-14C (CLS Cell Lines Service, Eppelheim, Germany) were cultured in Dulbecco's modified Eagle's medium Nutrient mixture F-12 HAM (DMEM/F12, Sigma-Aldrich) with 5% FBS, 2mM L-glutamine, 100 units/ml penicillin and 10 µg/ml streptomycin. When a confluence level of 80-90% occurred, accutase (Sigma-Aldrich) was utilized for subculturing. All cells were cultured at 37°C/5% CO_2 in a humidified atmosphere. A medium change was done every 2-3 days.

2.3 Immunocytochemistry

To evaluate the presence of gap junctions between hDPSC and tumor cells, a co-culture of hDPSC and UM-SCC-14C was performed. To this end, cells were seeded in 24-well plates (Greiner Bio-One) containing glass coverslips with a density of 5,000 cells/cm^2 at different hDPSC:SCC ratios (1:1, 1:2 and 1:3). Cell growth was allowed in DMEM/F12 with 10% FBS at 37°C until the cell culture was confluent. Fixation of the co-culture was acquired with an incubation in unifix (Klinipath, Duiven, The Netherlands) for 20 minutes at room temperature (RT). After washing in 1x phosphate buffered saline (PBS), the cells were incubated with a pure protein block solution (Dako, Glostrup, Denmark) for 20 minutes. Next, a 2 hour incubation at RT with primary rabbit monoclonal anti-connexin 43 antibody (1:1000, ab11370, Abcam, Cambridge, UK) happened in 1xPBS. The cells were washed afterwards with 1xPBS and incubated with Horse radish peroxidase labeled-goat-anti-rabbit IgG

secondary antibody (Dako) for 30 minutes. To accomplish connexin 43 staining, 3,3'-Diaminobenzidine (DAB) in chromogen solution (Dako) was added to the cell cultures for 7 minutes maximum. For counterstaining, an 8 minute incubation in hematoxylin was performed. Finally, the coverslips were mounted using anti-fade mounting medium (Dako) and visualized with Mirax Desk digital slide scanner (Zeiss, Oberkochen, Germany). Analysis was achieved with the Pannoramic Viewer 1.15.4 software (3DHistech, Budapest, Hungary). An isotype control was used to evaluate the quality of the staining procedure (1:1000, ab172730, Abcam).

2.4 Transmission electron microscopy

Using TEM, gap junctional intercellular communication was evaluated on an ultrastructural level. Therefore, hDPSC and UM-SCC-14C were seeded in 24-well plates (5,000 cells/cm^2, hDPSC:SCC ratios 1:1, 1:2 and 1:3) on Thermanox coverslips (Elektron Microscopy Sciences, Hatfield, PA) and fixated with 2% glutaraldehyde in 0.05 M sodium cacodylate buffer (Merck, Darmstadt, Germany) at 4°C after a confluency of 100% was reached. Twenty-four hours later, the fixated co-cultures were washed with 0.05 M sodium cacodylate buffer and 0.15 M saccharose before post-fixation occurred with 2% osmium tetroxide (Electron Microscopy Sciences) in 0.05 M sodium cacodylate buffer for 1 hour at RT. Next, the samples were dehydrated by exposure to acetone solutions with ascending concentrations (50% → 70% → 90% → 100% → 100%) and impregnated overnight with a 50/50 solution of 100% acetone and araldite (Fluka-Sigma-Aldrich). A 100% araldite solution was used to embed the samples. Ultrathin slices were made (±70 nm) with the ultramicrotome Ultracut 1 (Leica, Diegem, Belgium) and placed on 0.7% formvar-coated copper grids (Aurion, Essex, UK). The samples were contrasted with a 0.5% uranyl acetate and lead citrate solution in the EMAC20 contrasting system (Leica). For TEM, the Philips EM208 transmission electron microscope (Philips, Eindhoven, The Netherlands) provided with a Morada Soft Imaging System camera (Olympus, Tokyo, Japan) was utilized. Pictures were processed with iTEM-FEI software (Morada Soft Imaging System; Olympus, Tokyo, Japan).

2.5 Expression vector construction

To obtain HSV-tk expressing hDPSC, several steps were undertaken beginning with the production of the expression vector. The final utilized expression plasmid was acquired by transforming an already existing construct. This was accomplished by the incorporation of several multiple cloning sites (MCS), the replacement of the human sodium iodide symporter (hNIS) gene with the HSV-tk gene and the transfer of the construct to the final plasmid backbone (Figure 4).
Once the expression plasmid was manufactured, hDPSC were transfected to assess plasmid functionality.

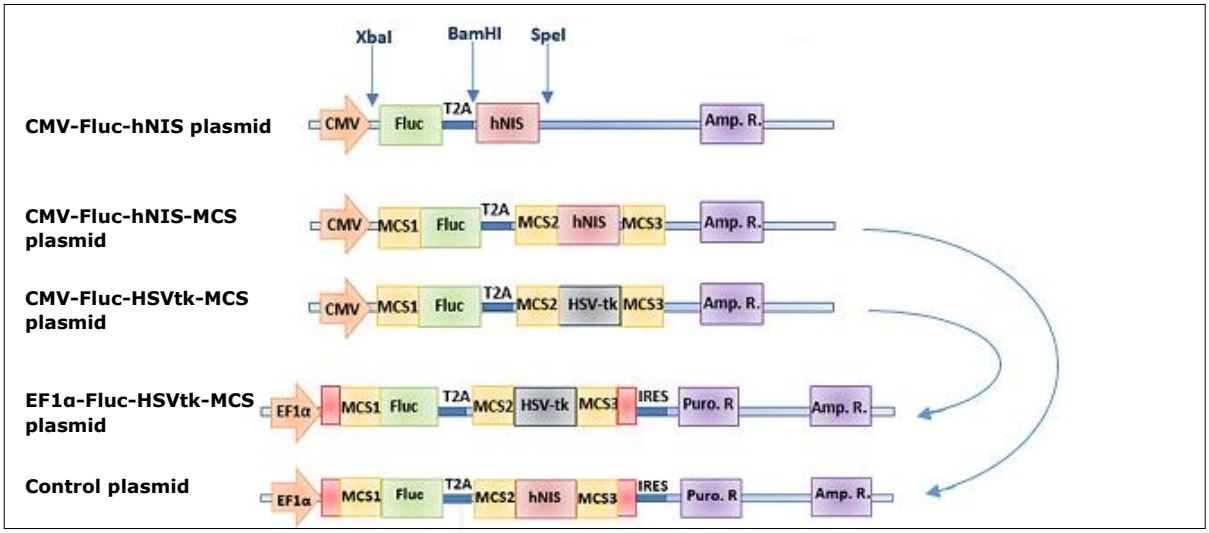

<u>Figure 4:</u> Steps for the production of an expression vector.
The fabrication of the expression plasmid was accomplished by the transformation of an already existing construct containing the firefly luciferase (Fluc) gene under control of the cytomegalovirus (CMV) promotor (CMV-Fluc-hNIS plasmid). To obtain the final expression plasmid, insertion of multiple cloning sites (MCS1-3) in XbaI, BamHI and SpeI sites was performed to make plasmid manipulation more plausible (CMV-Fluc-hNIS-MCS plasmid). Then, the human sodium iodide symporter (hNIS) gene was replaced by the Herpes Simplex Virus thymidine kinase (HSV-tk) gene (CMV-Fluc-HSVtk-MCS plasmid) and the entire construct was transferred to another backbone where gene expression is regulated by the human elongation factor 1-alpha promotor (EF1α) (EF1α-Fluc-HSVtk-MCS plasmid). In the control plasmid, hNIS was not replaced by the suicide gene. Plasmid selection was based on the presence of ampicillin and puromycin resistance genes (Amp. R. and Puro. R.). IRES: internal ribosome entry site, T2A: 2A peptide, two linker sequences that allow functional translation of downstream genes.

<u>2.5.1 Insertion of multiple cloning sites</u>

The expression plasmid was created by insertion of three MCS. These were obtained after the exposure of single stranded oligonucleotide sequences or primers (Table S1) to a series of descending temperatures (90°C-4 minutes, 70°C-10 minutes, 60°C-20 minutes, 50°C-30 minutes, 37°C-45 minutes, 10°C-60 minutes, 4°C-∞) to accomplish annealing. The concentration of the resulting MCS was measured by the Thermo Scientific NanoDrop 2000 (Isogen Lifescience, Temse, België) and the inserts were phosphorylated with T4 polynucleotide kinase in reaction buffer A, T4 Ligase buffer (1x) containing ATP (ThermoFisher Scientific). Incubation took place for 30 minutes at 37°C and 10 minutes at 70°C followed by sample purification with the Qiagen PCR purification kit prescribed in the producer's protocol (Qiagen, Venlo, The Netherlands).

Subsequently, insertion of the three different MCS took place at the XbaI, BamHI and SpeI sites, respectively. To this end, plasmid DNA (2 µg) was digested with these enzymes (1 µl, New England BioLabs, Ipswich, MA) at 37°C in their recommended buffer (New England BioLabs) depending on the used enzyme. Gel electrophoresis in a 0.8% agarose gel (Invitrogen, Aalst, Belgium) for 45 minutes at 135 eV was performed to evaluate plasmid digestion. DNA bands with the correct length (plasmid length is ±13,950 kb) were extracted and purified with the Qiagen Gel extraction kit according to the manufacturer's instructions.

Next, the plasmid was dephosphorylated and ligated using the Rapid DNA Dephos & Ligation Kit (Roche, Brussels, Belgium) as described in the company's protocol, the latter in the presence of phosphorylated inserts. For the negative control, ligation happened without the addition of the phosphorylated MCS.

2.5.2 Insertion of the suicide gene

After the presence of the MCS was confirmed, the HSV-tk gene was incorporated into the expression plasmid. The HSV1-SR39tk gene was kindly provided to us by Prof. dr. Gambhir from the University of Stanford, CA. First, the HSV-tk gene was amplified from the donor plasmid with polymerase chain reaction (PCR) amplification according to the instructions of the Platinum Pfx DNA polymerase kit (Invitrogen). In short, a PCR sample was made containing 1 ng HSV-tk plasmid, 1 mM $MgSO_4$ (Invitrogen), 0.3 mM dNTP mix (ThermoFisher Scientific), 0.3 µM forward and reverse primer (Table S1), 1x amplification buffer (Invitrogen), 1 unit Platinum Pfx DNA polymerase (Invitrogen) and autoclaved MilliQ. The PCR sample was exposed to flowing cycling conditions: 94°C for 5 minutes, [94°C for 15 seconds, 55°C for 30 seconds, 68°C for 2 minutes]x30 and 68°C for 10 minutes. The amplicon (HSV-tk gene) was isolated after gel electrophoresis for 45 minutes at 135 eV in a 1% gel with the Qiagen Gel extraction kit. Next, the construct containing all MCS (2 µg) and the HSV-tk amplicon were digested with NheI and AsiSI, (1 µl each, New England BioLabs) in cutsmart buffer at 37°C for 60 minutes followed by a 20 minute inactivation step of 80°C. Prior to ligation, the correct DNA band of the digested plasmid was isolated through gel electrophoresis and extraction out of a 0.8% gel followed by dephosphorylation. Amplicon phosphorylation took place as previously mentioned followed by PCR purification with the Qiagen PCR purification kit. Plasmid ligation was consistent with the Rapid DNA Dephos & Ligation Kit guidelines, as a negative control, no HSV-tk digest was added to the ligation mix.

2.5.3 Translocation towards an human elongation factor 1α promotor regulated plasmid

The final expression plasmid was obtained by the translocation of the generated constructs into an empty plasmid backbone (Figure 4). Therefore, a double digestion with PmeI and SbfI (New England BioLabs) was executed of the CMV-Fluc-hNIS-MCS and the CMV-Fluc-HSVtk-MCS plasmids in cutsmart buffer at 37°C for 1 hour. Digestion was inactivated with a 20 minute incubation period at 80°C. The new plasmid backbone containing the human elongation factor 1-alpha (EF1α) promotor was digested in a similar matter. Next, the digested plasmid backbone and the constructs (MCS1-Fluc-T2A-MCS2-hNIS/HSVtk-MCS3) where isolated by gel electrophoresis and extraction in a 0.8% gel. The digested plasmid backbone was dephosphorylated prior to ligation in the presence of the constructs. Either the construct containing hNIS or HSV-tk were added to the ligation mixture. As previously mentioned, gel extraction was performed with the Qiagen gel extraction kit, for plasmid dephosphorylation and ligation, the Rapid DNA Dephos & Ligation Kit was used.

2.5.4 Transformation of NEB 5-alpha Competent E. Coli

Plasmid amplification was accomplished by the transformation of NEB 5-alpha Competent E. Coli (New England BioLabs) through a 30 second heat shock at 42°C. As a negative control, transformation took place with the 'empty' plasmid construct (without inserts). In brief, 25 µl of NEB 5-alpha Competent E. Coli was thawed on ice for 30 minutes in the presence of 4 µl plasmid DNA prior to heat shock. Then, the bacteria were put back on ice for 5 minutes to complete the transformation procedure. E. Coli growth was allowed in 500 µl SOC outgrowth medium (New England BioLabs), first at 37°C/250rpm for 60 minutes, afterwards at 37°C overnight onto an ampicillin selection plate containing LB Agar (Invitrogen) and ampicillin (100 µg/ml, Roche).

2.5.5 DNA extraction and restriction analysis

To test the presence of all MCS and HSV-tk, E. Coli colonies were selected, transferred and additionally grown overnight in LB broth base (Invitrogen) at 37°C/250rpm to increase plasmid concentration. Next, plasmid DNA was isolated with the QIAprep Spin Miniprep (Qiagen) with the supplier's protocol and the DNA concentration was measured with the nanodrop. Enzymatic digestion and gel electrophoresis on a 1% agarose gel for 45 minutes at 135 eV allowed to verify the manifestation of MCS and HSV-tk insertion.

For MCS1, digestion was completed with HpaI (New England BioLabs) in cutsmart buffer 1 hour at 37°C. NheI, PmeI and AgeI (New England BioLabs) plasmid digestion was performed in cutsmart buffer for 1 hour at 37°C to test the presence of MCS2. Finally, AsiSI and PmeI were used to evaluate incorporation of MCS3 into the plasmid DNA. Also here, enzymatic DNA cleavage took place for 1 hour at 37°C.

Insertion of the HSV-tk gene in the plasmid was assessed through a double digestion with CIaI and SrfI (New England BioLAbs) in cutsmart buffer and a single digestion with KpnI (Roche) in Buffer SuRE/Cutbuffer L (Roche) with 100 µg/ml bovine serum albumin (BSA, New England BioLabs). Both enzymatic digestions took place for 60 minutes at 37°C prior to a 20 minute inactivation period at 65°C.

To verify if the MCS1-Fluc-T2A-MCS2-HSVtk-MCS3 or MCS1-Fluc-T2A-MCS2-hNIS-MCS3 constructs were inserted into the final plasmid backbone to accomplish the EF1α-Fluc-HSVtk-MCS or control plasmid respectively, restriction analysis was performed. To assess the production of the control plasmid, digestion with SpeI was done. To control the assembly of the EF1α-Fluc-HSVtk-MCS plasmid, digestion was achieved with XbaI. Both enzymatic digestions took place at 37°C for 60 minutes followed by a 20 minute incubation period at 80°C for inactivation. Each digest was compared with a 1 kb ladder (GeneRuler 1 kb Plus DNA ladder, ThermoFisher Scientific).

2.5.6 DNA sequencing

Final ligation products with the right restriction pattern were further examined with DNA sequencing to confirm the correct ligation. This was performed for the control plasmid and the EF1α-Fluc-HSVtk-MCS plasmid after plasmid amplification in E. Coli and plasmid DNA purification with the NucleoBond® Xtra Midi EF (Macherey-Nagel, Düren, Germany). The producer's protocol was applied for this purpose. In order to sequence the acquired plasmids, plasmid DNA (50 ng/µl) and sequence primers (5 pmol/µl, Table S1) were sent to the VIB Genetic Service Facility (Wilrijk, Belgium). The resulting genetic sequence was analysed for possible mutations.

2.6 human dental pulp stem cell transfection and luminescence assay

Plasmid functionality of three selected EF1α-Fluc-HSVtk-MCS and control plasmids was assessed after hDPSC transfection with the conventional Lipofectamine® 2000 reagent and protocol (Invitrogen). Briefly, hDPSC were seeded in a concentration of 10,000 cells/cm^2 in a black 96-well plate. After a culture period of 24 hours, the standard medium was replaced by FBS-free αMEM supplemented with

2 mM L-glutamine. Next, to accomplish transfection, hDPSC were incubated with plasmid DNA (100 ng) and lipofectamine (0, 2 ng/µl and 5 ng/µl) 1 hour later.
Firefly luciferase expression was evaluated by measuring the luminescence of the transfected hDPSC after D-luciferin addition (1:1, Promega One-Glo^{Tm} Luciferase Assay, Leiden, The Netherlands). A luminometer (FLUOstar Omega, BMG LABTECH, Ortenberg, Germany) was utilized to this extent and every condition was measured in duplo. For normalization, hDPSC of the same patient without the addition of the expression plasmid and lipofectamine were used.

2.7 Optimization of the 4-nitroquinoline-1-oxide rat model

Sixty-eight week old male Wistar rats (Janvier Labs, Le Genest-Saint-Isle, France) were retained under standard laboratory conditions, i.e. in a temperature-controlled room (±25°C) with a regulated 12 hour light-dark cycle and free access to food (natural chow diet) and drinking water. All experimental protocols involving the animals were conducted according to the guidelines for Animal Experiments and were approved by the Ethical committee of Hasselt University.

2.7.1 Treatment protocol

The carcinogen 4NQO (Sigma-Aldrich) was dissolved in propylene glycol (Sigma-Aldrich) to a final concentration of 5 mg/ml. After a two-week quarantine period, rats were divided into four groups; two control groups and two treatment groups. Both control cohorts contained three animals each, one group represented a native control, the other received a propylene glycol treatment three times a week. The treatment cohorts each consisted of 27 animals. The first treatment group received 4NQO via the drinking water (0.01 mg/ml) whilst the second was treated with 4NQO droplets (5 mg/ml) on the tongue three times a week. During every treatment session with propylene glycol or 4NQO, animals were anaesthetized with 3 to 4.5% isoflurane (Isoflo, Abbott, Belgium) in pure oxygen with a flow rate of 2 l/minute. The mouth was opened using a pincer and the solution was administrated with a paint-brush on the tongue.

2.7.2 Perfusion and tissue isolation

To assess the disease progression, three animals of each treatment group were sacrificed at the end of every month starting from the onset of 4NQO administration. At month nine, all the remaining animals were sacrificed. At these time points, death was induced with an overdose of Nembutal (60 mg/kg bodyweight i.p.; CEVA Logistics, Belgium) followed by transcardial perfusion with ringer solution containing heparin. Next, perfusion continued with a 4% paraformaldehyde solution (PFA). After perfusion, the head of every animal was dissected and preserved in a 4% PFA solution. Liver specimens were taken when lesions were observed.

2.7.3 Masson's Trichrome staining

Tumor development was histologically examined with Masson's Trichrome staining. Several 5 µm thin paraffin slices of tongue tissue were made. First the specimens were deparaffinised to water by the incubation in 3 xylene baths (VWR, Leuven, Belgium), 3 baths of 100% denaturated alcohol (VWR) and one bath of 75% denaturated alcohol. Afterwards, the histological slides were washed in 2 baths of distilled water. All incubation periods had a length of 2 minutes. For nuclear staining, the

slides were stained with a Mayer's haematoxylin solution for 8 minutes prior to a 30 minute washing step in tap water and a 2 minute washing step in distilled water. Next, the specimen were placed for 5 minutes consecutively in a Ponceau-Fuchsin bath, a 1% phosphomolybdic acid bath, a aniline blue bath, a 1% phosphomolybdic acid bath and a 2 minute bath in 1% acetic acid. In-between, the samples were washed with distilled water. After this staining procedure, the slices were impregnated with 100% denatured alcohol (4 baths, 2 minutes each). Dehydration was accomplished with a 4 minute incubation in an alcohol pro-analyse (VWR) bath followed by 3 xylene baths of 4 minutes. Finally, DPX mounting medium was used to seal the specimens. The tissue samples were analysed with the Mirax Desk digital slide scanner and visualized with the Pannoramic Viewer 1.15.4 software.

2.7.4 Immunohistochemistry

Immunohistochemical staining for different markers on the tongue tissue after 4NQO exposure was also performed. The paraffin sections selected for staining presented macroscopic lesions. Tissues were deparaffinised to water as previously mentioned prior to heat-induced antigen retrieval in citrate buffer (Dako). A microwave was used for this cause to heat the samples for 15 minutes at 480 W with 2 minute intervals every 5 minutes. Next, the samples were incubated for 20 minutes at RT with peroxidase blocking solution (Dako) to diminish endogenous peroxidase activity. Afterwards, samples were washed with 1xPBS. Non-specific binding of the utilized antibodies was blocked with a 20 minute incubation in a pure protein blocking solution (Dako). Staining of the tissue sections occurred for several antigens, incubation with the primary antibodies (Table 1) occurred overnight at 4°C. Subsequently, samples were incubated for 30 minutes with goat-anti-rabbit or goat-anti-mouse horse radish peroxidase labelled IgG secondary antibody (Dako) depending on the primary antibody used. Prior to DAB incubation (1-7 minutes) with the DAB envision kit (Dako), the tissue sections were washed with 1xPBS. Counterstaining was obtained with haematoxylin as stated above and samples were enclosed with aquatex mounting medium. Analysis was carried out using a Mirax Desk digital slide scanner with Mirax scan software.

Table 1: Primary antibodies utilized for immunohistochemistry on tongue tissue.

Antigen	Host	Dilution	Ref. Nr.	Company
Cytokeratin 19 (Clone BA17)	Mouse	1:50	ab7755	Dako, Glostrup, Denmark
Desmin (Clone 33)	Mouse	RTU	N1526	Dako, Glostrup, Denmark
Connexin 43	Rabbit	1:1000	ab11370	Abcam, Cambridge, UK
MAGEA3/MAGE3	Rabbit	1:250	abc468	Merck Millipore, Overijse, Belgium

Abbreviations: RTU: ready to use solution, MAGEA3: Melanoma-associated antigen 3.

3. RESULTS

The aim of this internship was to analyse if hDPSC are valuable mediators in suicide gene therapy. In order to provide a basis to indicate if indeed this might be the case, different aspects were evaluated. First, the capacity of gap junction formation between hDPSC and tumor cells was assessed by performing immunocytochemistry and electron microscopy. Afterwards, an expression vector was designed to make hDPSC transfection and future transduction possible. Furthermore, the 4NQO rat model was optimized and valued for upcoming *in vivo* experiments.

3.1 human dental pulp stem cells and tumor cells form gap junctions

A vital aspect of stem cell-mediated suicide gene therapy is the presence of gap junctions between the stem cells and the surrounding tumor cells. The passage of phosphorylated GCV from the hDPSC to the tumor cells and the resulting bystander effect is relying on this key element. Hence, gap junction formation was analysed in co-cultures of hDPSC and UM-SCC-14C tumor cells. To indicate the presence of gap junctions, immunocytochemistry was conducted against connexin 43, a common, widely expressed constituent of gap junctions (39). Transmission electron microscopy was applied to confirm the data ultrastructurally.

3.1.1 Connexin 43 expression is present in tumor and human dental pulp stem cell co-cultures

Morphologically, a clear distinction could be made between the hDPSC and tumor cells. The hDPSC could be recognized as fibroblast-like to polygonal-like shaped cells, whilst the tumor cells were smaller and more circular-shaped (Figure 5). Diaminobenzidine staining revealed connexin 43 expression on both cell types. Moreover, the distribution of connexin 43 on the cell surface was observed to be polar and present at sites where cells were concentrated. Throughout the cell culture, colouration took place in hDPSC-dense regions, tumor cell-dense regions and areas where the two cell types bordered each other. All co-cultures obtained from different independent hDPSC donors delivered similar results, variation in cell ratios did not influence the presence of connexin 43 as well (Figure 5).

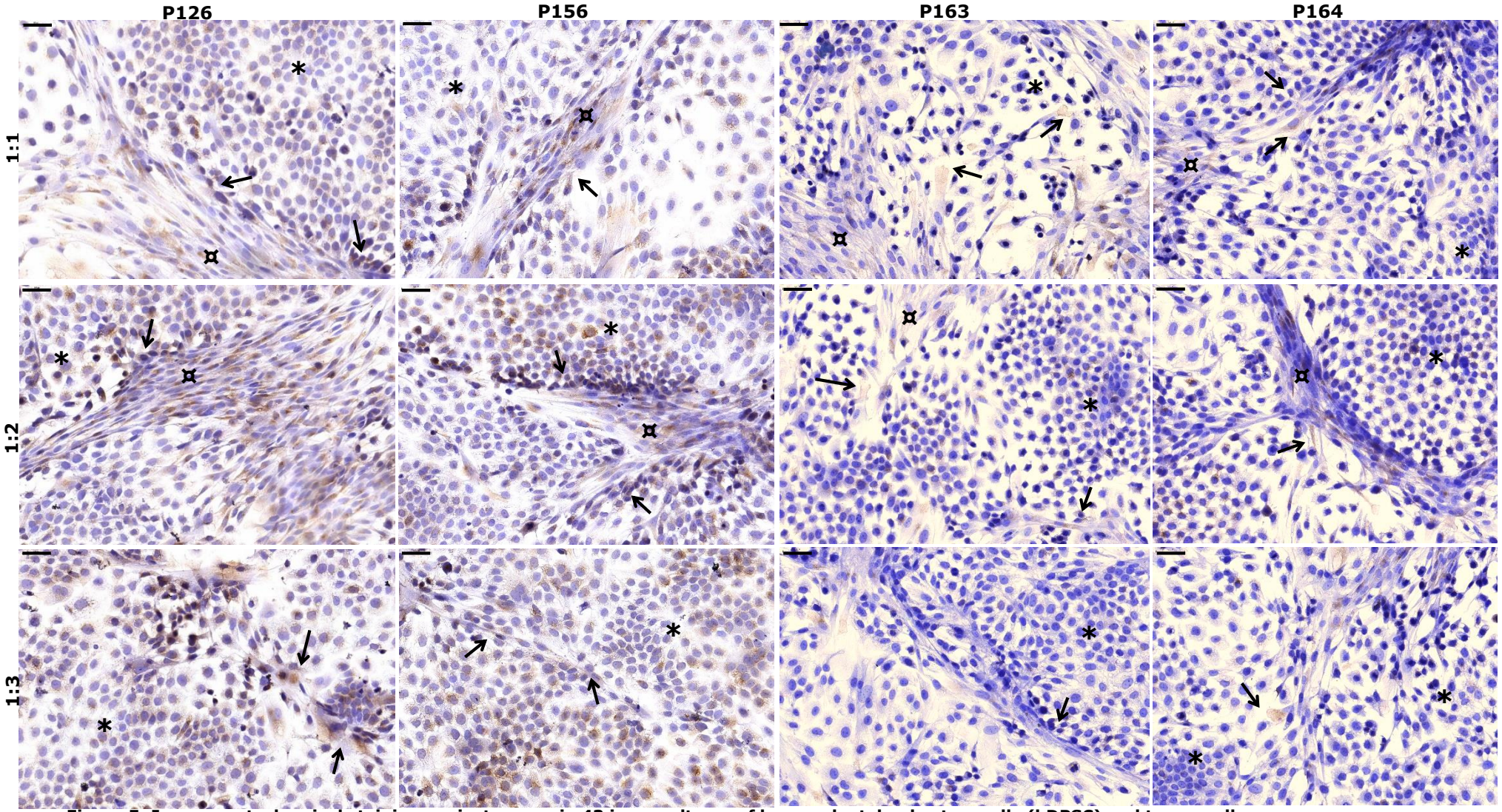

<u>Figure 5:</u> Immunocytochemical staining against connexin 43 in co-cultures of human dental pulp stem cells (hDPSC) and tumor cells.
Tumor cells (UM-SCC-14C) and hDPSC of four different independent donors (p126, p156, p163 and p164) were seeded with a density of 5,000 cells/cm^2 at different hDPSC:SCC ratios (1:1, 1:2 and 1:3). Cell growth in the co-cultures was allowed in DMEM/F12 medium with 10% FBS until the cultures became confluent. The presence of connexin 43 was analysed with a primary rabbit monoclonal anti-connexin 43 antibody (1:1000, Abcam) prior to DAB incubation. Connexin 43 staining arose in tumor cell-rich regions (*), hDPSC-dense regions (¤) and regions where the two cell types aligned (arrow). The pictures are representative for the obtained results. (Scale bar= 50 µm).

3.1.2 Cell interactions contain gap junctions in tumor and dental pulp stem cell co-cultures

On an ultrastructural level, a clear distinction between the two cell types could be made (Figure 6). hDPSC were characterised by a large spherical and euchromatic nucleus containing one or two prominent nucleoli. The extended cell cytoplasm could be divided in a perinuclear zone rich of organelles as rough endoplasmic reticulum and Golgi apparatus and an electron-lucent peripheric region without cell organelles. Mitochondria in the perinuclear zone showed an elongated morphology. Electron-lucent vesicles were also found in the cytoplasm (Figure 6B-C).

The squamous tumor cells had a very distinct morphological appearance. They were smaller and had a rough cell surface with several small cytoplasmic extensions. The large round cell nucleus contained prominent nucleoli. Cell organelles were scattered throughout the cell body. Within the cytoplasm, mitochondria, rough endoplasmic reticulum and Golgi complexes were observed (Figure 6A).

Cell-cell contacts were visible between neighbouring tumor cells (Figure 6A) or hDPSC (Figure 6B). Frequently, electron-dense membrane regions were acknowledged at these cell contacts. Cell interaction between the two different cell types were also realized (Figure 6C). This was detected between cytoplasmic extensions of hDPSC and the squamous tumor cells. Some of these cell contacts showed an increased membrane density (Figure 6D).

Taken together, the connexin 43 expression and the typical occurrence of the electron-dense membrane regions indicate gap junction formation between tumor cells, hDPSC and both cell types.

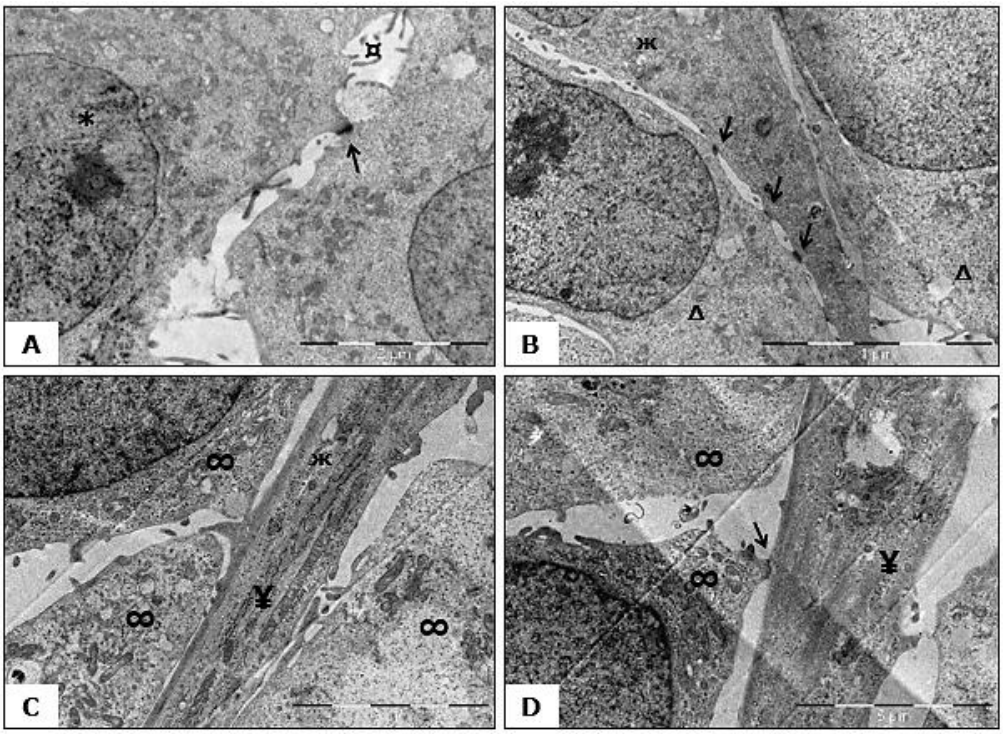

Figure 6: Transmission electron microscopy of tumor and human dental pulp stem cell co-cultures. UM-SCC-14C and human dental pulp stem cells (hDPSC) were seeded with a density of 5,000 cells/cm^2 at a ratio of 1:1, 1:2 and 1:3 (hDPSC:SCC). Growth conditions were similar as stated in Figure 5. **(A)** Tumor cells had small cytoplasmic extensions (¤), a large prominent nucleus with heterochromatic regions (*) and numerous cell organelles distributed over the cytoplasm. Electron-dense regions between tumor cells were present (arrow). **(B)** Cell interaction between hDPSC were also observed. At places of cell contact, electron-dense membrane regions were witnessed (arrows). The extended cytoplasm contained electron-lucent vesicles (Δ) and perinuclear located cell organelles including elongated mitochondria (Ж). **(C)** Cytoplasmic extensions of hDPSC (¥) made contact with SCC tumor cells (∞), **(D)** membrane thickening appeared at these sites (arrow). The pictures are representative for the acquired results. (Scale bar= 2 µm **(A)**, 1 µm **(B)** and 5 µm **(C-D)**).

3.2 Restriction analysis confirmed the generation of the expression vector

To accomplish HSV-tk expression in hDPSC, an expression vector was designed. During the course of this expression plasmid production, several restriction analyses were performed in order to utilize the correct expression plasmid for additional manipulation. To acquire the final and control plasmid, three MCS were inserted into the plasmid DNA prior to the insertion of the suicide gene. Next, Fluc and HSV-tk or Fluc and hNIS were placed under control of the EF1α promoter (Figure 4).

3.2.1 Insertion of the multiple cloning sites

Ampicillin selection after E. Coli transformation indicated proper ligation of the MCS into the plasmid backbone. The negative control with the 'empty' plasmid construct (without inserts) did not show any colonies (Figure 7).

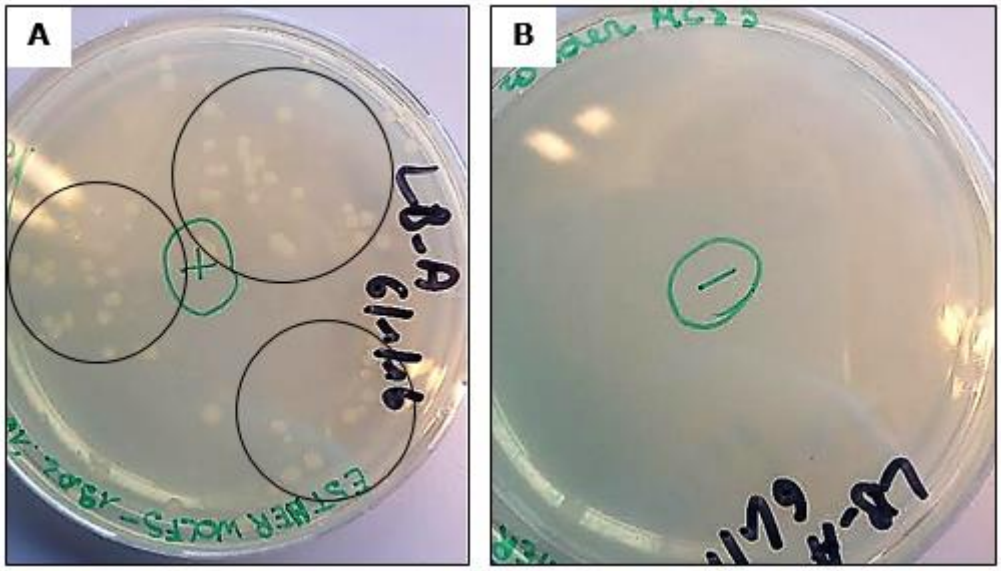

Figure 7: Example of an E. Coli transformation and culture.
(A) E. Coli transformation after plasmid ligation in the presence of the insert (here multiple cloning site three (MCS3)). Due to the complementary sticky ends of the insert, the plasmid could ligate where after it was taken up by the E. Coli during the heat shock procedure. E. Coli colonies were formed overnight on an ampicillin selection plate (Encircled). **(B)** Negative control. Here, heat shock was performed after ligation induction without the insert. As a result of the absence of MCS, the plasmid backbone was not able to ligate. Therefore, no colonies were formed overnight because of ampicillin selection. The pictures are a representative for the obtained results during MCS insertion.

Insertion of the MCS was tested with a HpaI digestion for MCS1, a double digestion with NheI and AgeI or PmeI and NheI for MCS2 and a digestion with AsiSI and PmeI for MCS3 (Figure 8E). Restriction analysis with HpaI revealed two bands of ±10.8 kb and ±3.1 kb in practically all tested clones, which indicates the presence of MCS1 (Figure 8A). After the ligation of MCS2 in the plasmid, digestion with NheI and AgeI indicated MCS2 insertion with two bands of ±7.8 kb and ±6.2 kb (Figure 8B). The ligation of MCS2 in the presence of MCS1 was confirmed with PmeI and NheI digestion, all clones presented the expected band lengths; ±12 kb and ±1.8 kb (Figure 8C). Restriction analysis with PmeI and AsiSI after MCS3 ligation indicated insertion of MCS3 in the plasmid containing MCS1. Five clones displayed the correct lengths; ±10.2 kb and ±3.8 kb (Figure 8D).

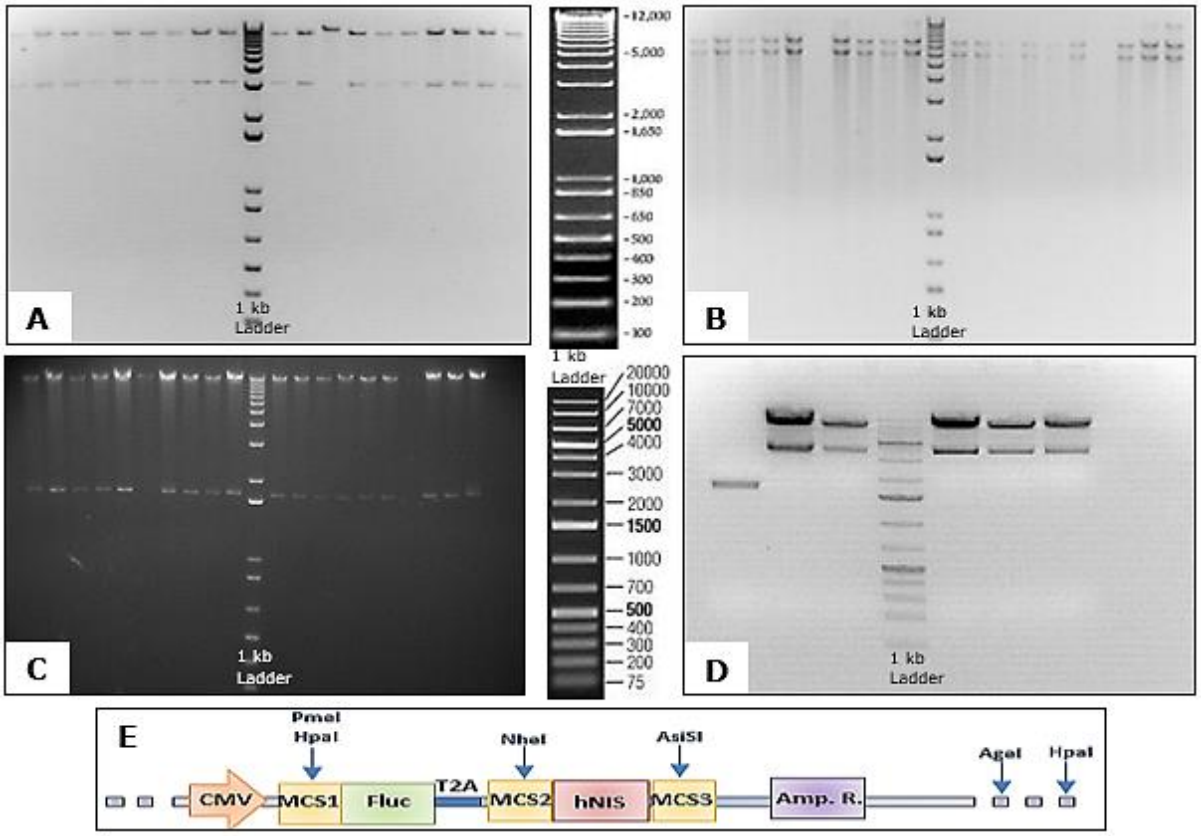

Figure 8: Restriction analysis of the CMV-Fluc-hNIS plasmid after multiple cloning site insertion.

(A) After HpaI digestion, the correct DNA fragment lengths ±10.8 kb and ±3.1 kb were obtained, indicating multiple cloning site (MCS)1 insertion. **(B)** Ligation of MCS2 was tested by a double digestion with NheI and AgeI. The expected DNA bands with lengths ±7.8 kb and ±6.2 kb were detected. **(C)** PmeI and NheI digestion confirmed MCS2 manifestation. All clones displayed two bands with a length of ±12 kb and ±1.8 kb. **(D)** The insertion of MCS3 was analysed with PmeI and AsiSI digestion. In five clones, the two bands with a length of ±10.2 kb and ±3.8 kb were present corresponding with the expected lengths. **(E)** Schematic representation of the restriction sites of HpaI, NheI, AgeI, PmeI and AsisI in the CMV-Fluc-hNIS-MCS plasmid.

3.2.2 Insertion of the suicide gene into the expression plasmid

For the insertion of the suicide gene into the designed expression plasmid containing the three MCS, PCR amplification was performed first (Figure 9A). Gel extraction of the HSV-tk gene with a length of ±1.2 kb was performed prior to ligation. Next, restriction analysis with CIaI and SrfI or KpnI revealed insertion of the suicide gene into the expression plasmid for several clones (Figure 9B-D).

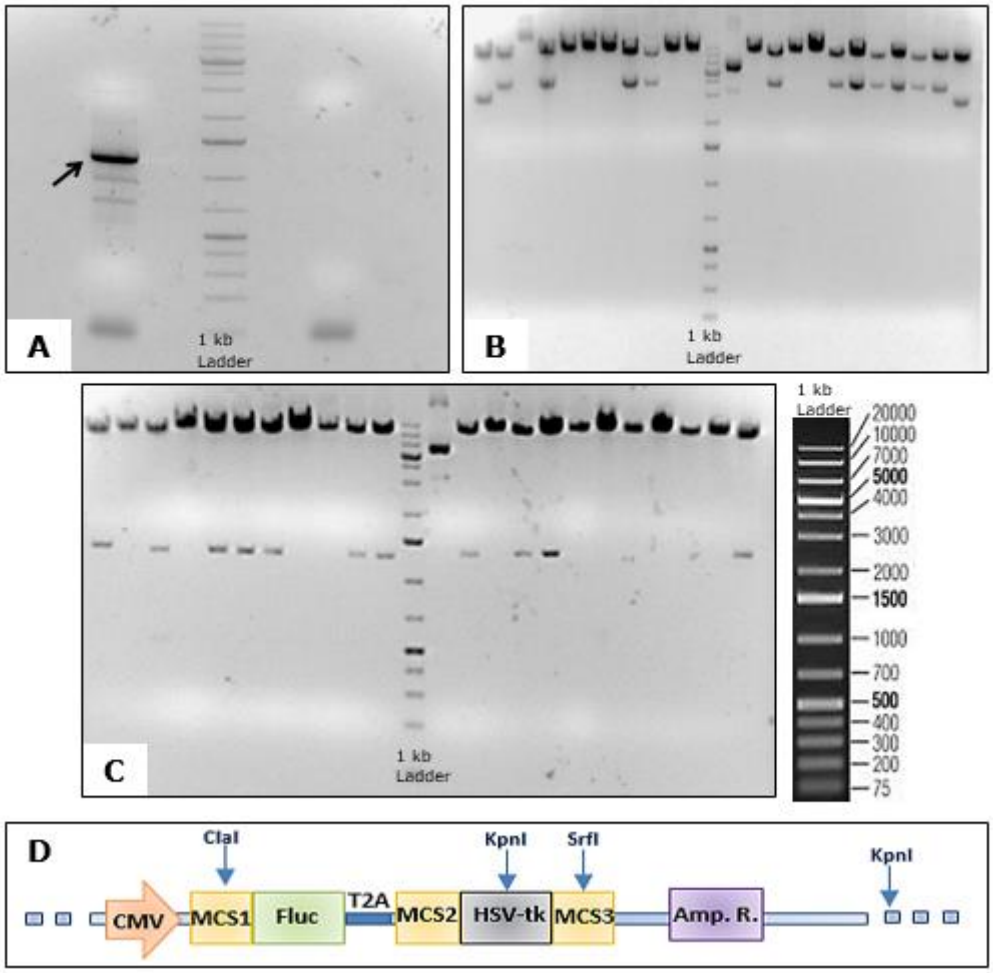

Figure 9: Suicide gene isolation and restriction analysis after HSV-tk ligation.
(A) Polymerase chain reaction (PCR) amplification resulted in the isolation of the HSV-tk suicide gene (arrow). **(B)** Restriction analysis after HSV-tk ligation with SrfI and CIaI revealed the insertion of the suicide gene in several clones. The lengths of ±10.2 kb and ±2.9 kb were acknowledged. **(C)** KpnI digestion confirmed the insertion of HSV-tk in the expression plasmid for some clones (±11.8 kb and ±1.3 kb). When only one DNA band was observed, HSV-tk was absent in the plasmid DNA. **(D)** Schematic representation of the restriction sites of SrfI, CIaI and KpnI in the CMV-Fluc-HSVtk-MCS plasmid.

3.2.3 Translocation towards an human elongation factor 1α promotor regulated plasmid

To produce the final EF1α-Fluc-HSVtk-MCS and control plasmid (Figure 4), Fluc and HSV-tk or Fluc and hNIS respectively were placed under the control of the EF1α promotor. To accomplish the generation of these final plasmids, the CMV-Fluc-hNIS-MCS plasmid, the CMV-Fluc-HSVtk-MCS plasmid and the backbone plasmid were digested with PmeI and SbfI first (Figure 10A).

After ligation and E. Coli transformation, restriction analysis was performed. Digestion with SpeI showed correct construct insertion in the control plasmid, as the lengths of the DNA bands were ±7.6 kb and ±3.8 kb (Figure 10B left side). XbaI digestion of the EF1α-Fluc-HSVtk-MCS samples revealed the expected lengths (±5.8 kb and 4.8 kb) for most clones (Figure 10B right side). When the constructs were absent in the plasmid backbone, a length of ±7.6 kb was observed (Figure 10B).

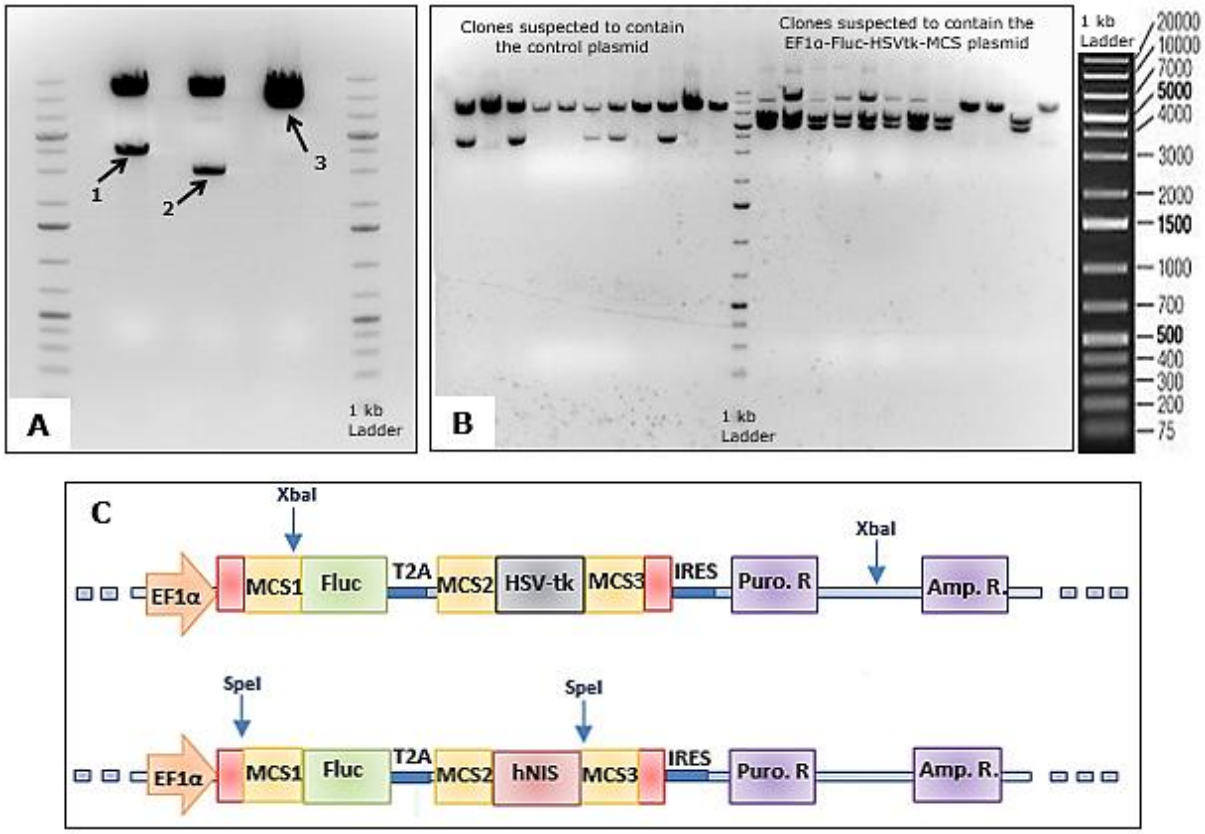

Figure 10: Construct isolation and restriction analysis of the control or EF1α-Fluc-HSVtk-MCS plasmid. **(A)** After PmeI and SbfI digestion, the MCS1-Fluc-T2A-MCS2-hNIS-MCS3 (arrow 1) and the MCS1-Fluc-T2A-MCS2-HSVtk-MCS3 (arrow 2) constructs were isolated after gel electrophoresis. The plasmid backbone was digested to make proper ligation possible (arrow 3). **(B)** SpeI (left side ladder) and XbaI digests (right side ladder) of the control plasmid and EF1α-Fluc-HSVtk-MCS plasmid respectively. SpeI digestion revealed DNA bands with a length of ±7.6 kb and ±3.8 kb, indicating the obtainment of the control vector. XbaI digestion of the EF1α-Fluc-HSVtk-MCS plasmid displayed the expected results as well. DNA bands with a length of ±5.8 kb and 4.8 kb were visible. When the plasmid backbone was empty, a length of ±7.6 kb was observed. **(C)** Schematic representation of the restriction sites of SpeI and XbaI in the control and EF1α-Fluc-HSVtk-MCS plasmid respectively.

3.3 The designed expression plasmid was functional

After the designed expression vector was obtained, sequencing and a luminescence assay were performed to assess gene functionality. Sequencing indicated the production of the desired constructs, yet in three clones, a mutation in HSV-tk was found (data not shown).

The luminescence assay confirmed Fluc expression and functionality for one EF1α-Fluc-HSVtk-MCS clone after a transfection period of one night with 5 ng/µl lipofectamine. No Fluc activity was detected for any of the control plasmid clones (Figure 11).

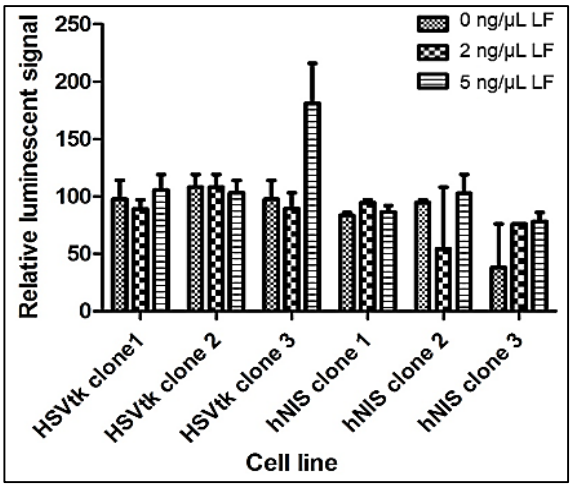

Figure 11: Luminescence assay.
human dental pulp stem cells (hDPSC) were transfected overnight with the control or EF1α-Fluc-HSVtk-MCS plasmid (three hNIS and HSVtk clones respectively) using different concentrations lipofectamine (LF). Only one clone confirmed expression vector functionality. Data is represented as mean ± standard error of the mean. Normalization occurred with DNA and LF-free hDPSC.

3.4 Chronic 4-nitroquinoline-1-oxide administration resulted in oral dysplasia in rats

For future analysis of hDPSC-mediated suicide gene therapy, a representative animal model for human OSCC was optimized. To induce carcinogenesis, rats were exposed to 4NQO for nine months through the drinking water or via treatment sessions three times a week. After perfusion and MRI, tongue tissue was isolated for Masson's Trichrome staining (Figure 12) and immunohistochemistry direct against several markers (Figure 13).

Healthy tongue tissue was characterised by a distinctive keratinized stratified squamous epithelium. The dorsal area of the tongue was specialized with long and intensely keratinized filiform papillae. Basal epithelial cells were columnar shaped and strongly attached to the basement membrane/basal lamina. Large epithelial processes known as rete ridges, projected in the underlying loose connective tissue of the lamina propria. Ventral in the lamina propria, underlying striated muscle fibres in the submucosa were observed (Figure 12A). The oral epithelium at lesion site of a 4NQO-treated rat presented a broad-based exophytic outgrowth with an atypical shape of the rete processes (Figure 12B). Loss of a clear basal lamina and cell differentiation was apparent (Figure 12C arrows). In addition, cell layer specificity was lost. Cellular invasion in the lamina propria of the circumvallate papillae was also detected (Figure 12C-D).

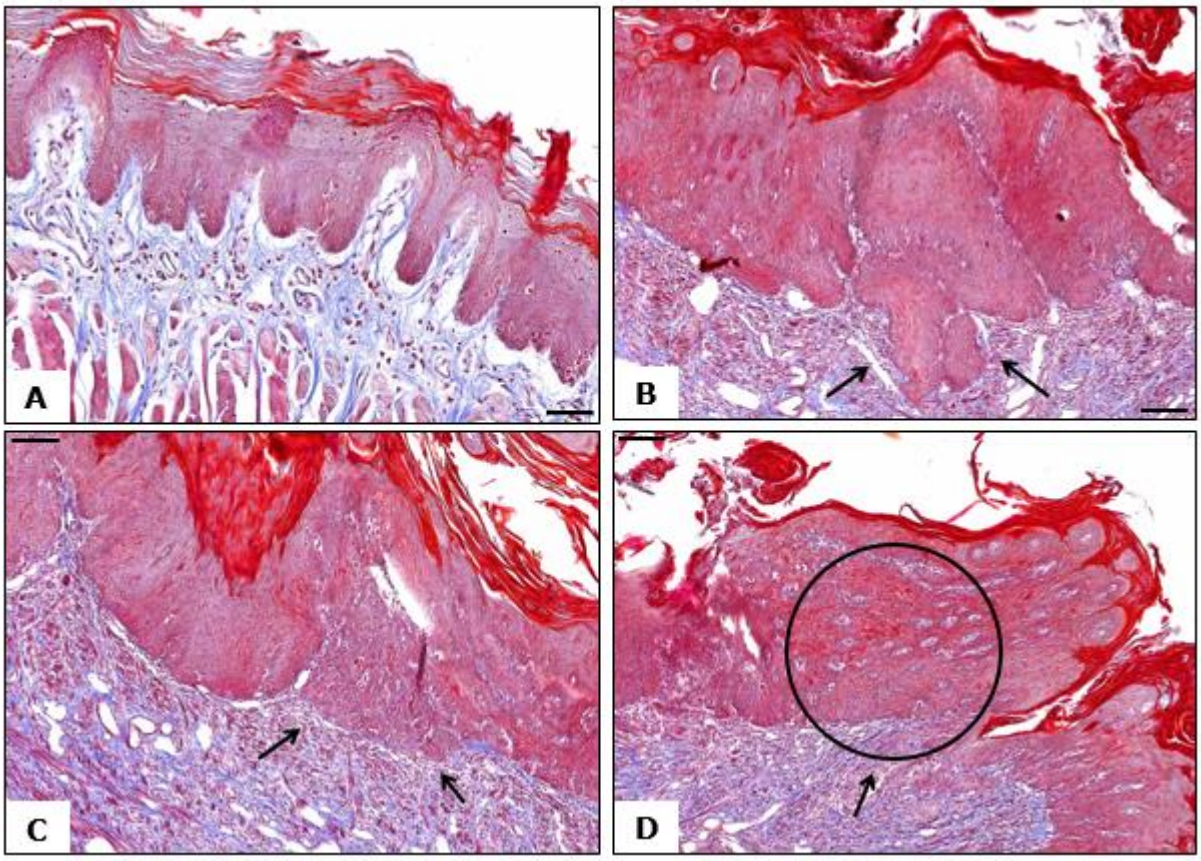

Figure 12: Masson's trichrome staining of healthy and abnormal tongue tissue.
(A) Healthy tongue tissue of a 4-nitroquinoline-1-oxide (4NQO)-treated rat. A typical keratinized stratified squamous epithelium with rete ridges dorsal of the lamina propria was found. **(B)** Tissue section from the lesion site presented a different morphology. Rete processes were abnormally shaped (arrows). **(C)** Loss of a distinct basal lamina and cell differentiation was observed (arrows) **(D)** and the lamina propria of the circumvallate papillae showed the presence of a cell mass (arrow). (Scale bar= 50 µm **(A)** and 100 µm **(B-D)**).

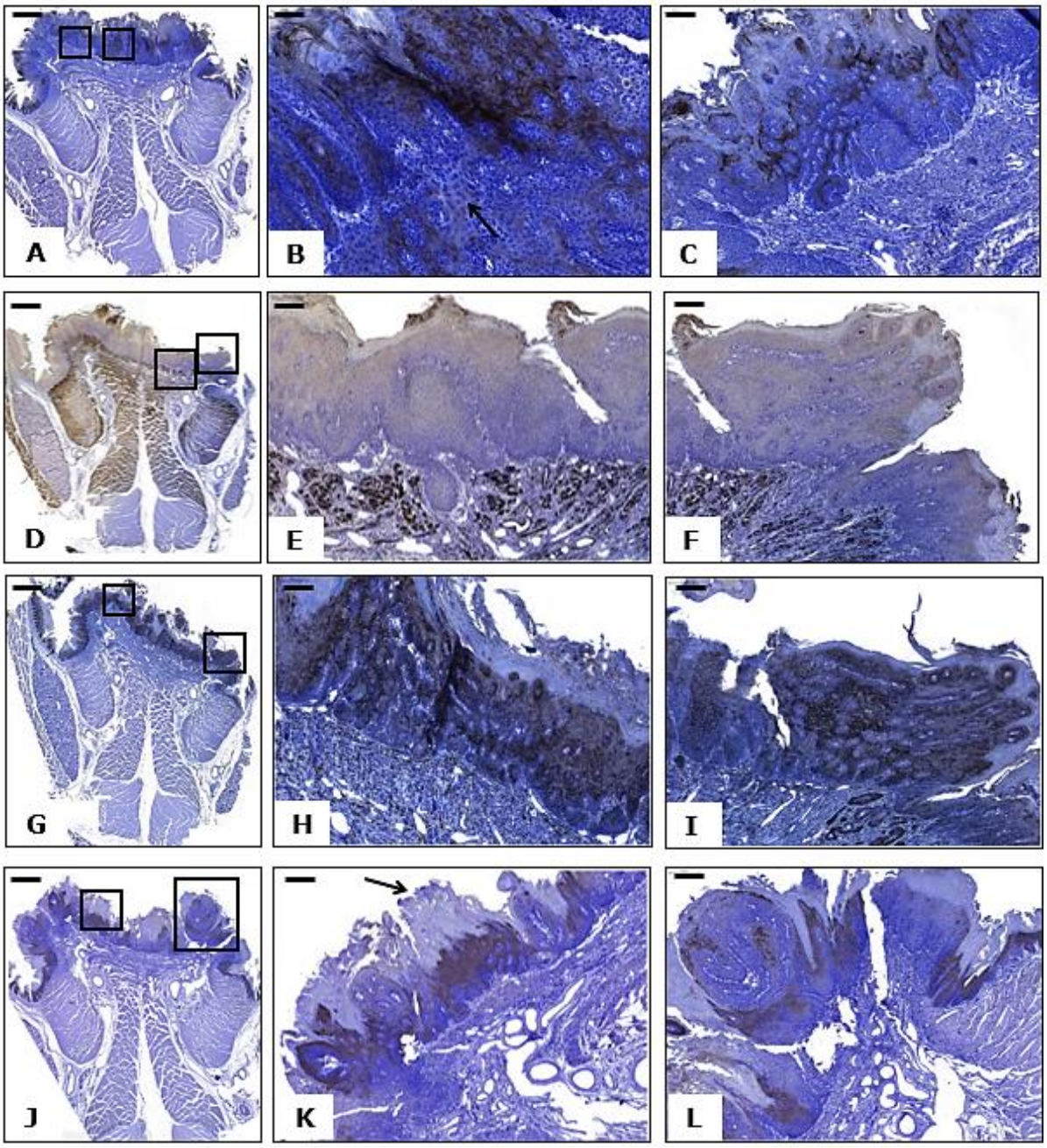

Figure 13: Immunohistochemistry of tongue lesions of a 4-nitroquinoline-1-oxide (4NQO)-treated rat. The observed tongue tissue was obtained from a rat treated with 4NQO for eight months. Tongue tissue was collected for cytokeratin 19, desmin, connexin 43 and melanoma-associated antigen 3 (MAGEA3) staining. Overview of the tongue tissue is represented in the left column, close-ups of the indicated zones are listed in the two right columns. **(A-C)** The lesion was cytokeratin 19 positive, pattern loss of the rete ridges was observed (arrow). **(D-F)** Desmin expression was found in muscle tissue. Aspecific keratin staining was present. **(G-H)** Strong connexin 43 reactivity existed in the oral epithelium, the cell mass of the circumvallate papillae and small saliva glands. **(J-L)** The oral epithelium of the tongue and the cell border of the circumvallate papillae expressed MAGEA3. Hyperkeratosis was detected (arrow). (Scale bar= 1000 µm **(A,D,G and J)**, 50 µm **(B)**, 100 µm **(C, E-F and H-I)** and 200 µm **(K-L)**).

The observed dysplastic lesion was characterized by immunohistochemical staining. Tissue sections were evaluated for the presence of cytokeratin 19, desmin, connexin 43 and the malignant transformation marker melanoma-associated antigen 3 (MAGEA3). Immunohistochemical evaluation revealed cytokeratin 19 expression in the basal cell layer and the stratum spinosum of squamous epithelial cells at the lesion site (Figure 13A-C). Tongue tissue after chronic 4NQO administration also presented loss of the normal arrangement of the rete ridges. Loss of cell differentiation and epithelial cell specificity was present (Figure 13B, arrow).

Immunoreactivity against desmin was related with the presence of smooth and striated muscle tissue (Figure 13D-F). A ventral epithelial outgrowth in the lamina propria between the muscle fibers was apparent (Figure 13E). Diaminobenzidine staining at the keratin borders indicated aspecific staining. The dysplastic tongue tissue also showed a positive reactivity for connexin 43. Glandular and stratified squamous epithelium strongly expressed connexin 43 (Figure 13G-I). The stainability for connexin 43 decreased in the lamina propria. Dorsal epithelial outgrowth was found (Figure 13H). Staining of cell mass in the centre of the circumvallate papillae indicated the occurrence of connexin 43 (Figure 13I).
Evidence of malignant transformation was identified with MAGEA3 antigen staining (Figure 13J-L). The spinous cell layer showed a high reactivity for MAGEA3 including the epithelial cell border of the circumvallate papillae. At the lesion site, hyperkeratosis was observed (Figure 13G-H, arrow).

In conclusion, immunohistochemical analysis revealed dysplasia of the tongue epithelium characterized with abnormal differentiation, loss of the epithelial cell layers, dorsal and ventral epithelial outgrowth and an increase in tongue keratinization. A distinctive metastatic cell mass in the underlying lamina propria was not detected yet. However, loss of a clear basal lamina was already specified at the lesion site. This data therefore indicates that chronic 4NQO administration can result in invasive tumor development.

4. DISCUSSION

In order to develop hDPSC-mediated suicide gene therapy, it is essential to gain more insight into the interaction of these stem cells with tumor cells and their potency to be used as a gene carrier. In this research project, the main focus was to identify whether hDPSC were capable to mediate tumor cell death through the bystander effect and to develop a suitable animal model to represent human OSCC for future *in vivo* experiments. To evaluate the possible occurrence of the bystander effect, gap junction formation between hDPSC and OSCC cells was analysed first. Next, an expression vector was designed containing the HSV-tk suicide gene and Fluc to make stem cell tracking at a later stage possible. For the optimization of the OSCC rat model, tumor development was evaluated in an eight month long 4NQO-treated rat.

4.1 Morphological and ultrastructural analysis of co-cultures

Our results demonstrate for the first time that hDPSC are able to interact with tumor cells, in particular a human OSCC cell line. Analysation of hDPSC and OSCC co-cultures demonstrated the expression of connexin 43 at the plasma membrane of both tumor cells and hDPSC. Connexin 43 expression was indicated to be polar and located on cells present in cell-dense regions. Cell-cell interactions with connexin 43 expression were observed between stem cells, tumor cells and both cell types, all indicating possible gap junction formation. Connexin 43 expression by OSCC tumor cells and hDPSC individually was already previously described (40-42). Observed slight variations of connexin 43 expression in the co-cultures between stem cells and stem cells with tumor cells can be explained by patient variability. A decrease in connexin 43 expression of hDPSC might be elucidated by the age of the stem cell donor. Quantitative real-time PCR data described by Muramatsu et al. indicated reduced connexin 43 transcription associated with aging (43).

Although the presence of connexin 43 is a substantial indicative for gap junctions between adjacent cells, its surface expression does not always guarantee the formation of functional gap junctions (44, 45). Possibly by the lack of proper connexin 43 clustering needed for the establishment of connexons or the formation of hemichannels (46-48). Therefore, to confirm that the detected connexin 43 expression represents the presence of gap junctions, TEM was performed.

Morphologically, hDPSC showed similar ultrastructural characteristics as described previously by our research group (49, 50). These cells had a typical perinuclear distribution of cell organelles, a large round nucleus with predominant euchromatic regions and one to two well-developed nucleoli (51). An atypical feature found in the co-culture system was the large amount of electron-lucent vesicles and the presence of large elongated mitochondria in the cytoplasm of hDPSC. The appearance of these mitochondria might indicate mitochondrial fusion, which is associated with cellular stress. In this specific research, increased fusion may be the consequence of the reduction of glucose by tumor cell outgrowth, leading to starvation of the hDPSC. As a response, mitochondria become more fused to maximize oxidative phosphorylation and proteins or lipids are used as a new energy source (52). This lipid metabolization might also explain the abundant number of electron-lucent vesicles in the cell cytoplasm of the hDPSC (53).

The squamous tumor cells presented a different morphology. Cells had a more irregular shape, with cell organelles scattered over the entire cytoplasm. A prominent nucleus was present, characterised by large nucleoli. The rather rough cellular surface of the tumor cells was in correspondence with previous findings of Leek H. et al. (54) and Tanaka et al. (55). Both research groups exposed the presence of microvilli at the cell surface of OSCC which were sometimes short and stubby and varying in number (54, 55).

Ultrastructural analysis of the cellular interactions between cells showed enhanced electron density in stretches of cell membranes of two close neighbouring cells. In combination with the previously acknowledged connexin 43 expression, one could state that these electron-dense regions are gap junctions. Ultrastructurally, gap junctions cannot be mistaken for other important specialized cellular structures such as the desmosome and hemidesmosome. Both adhesion structures arbitrate mechanical stability and contain transmembrane proteins, an intracellular plaque of desmoplakin and tonofilaments (56, 57). Squamous cell carcinomas have been found to be characterised by a rich network of desmosomes between adjacent tumor cells (54, 55). Therefore, the electron-dense membranes could be interpreted as desmosomes, at least between neighbouring tumor cells.
Morphologically however, the appearance of these junctional complexes is larger than the observed structures due to the electron-dense long bundles of tonofilaments surrounding the desmosomal plaques (54, 57). The width of the intracellular space at the site of a desmosome is generally found to be wider (±30 nm) as well. The intracellular space between opposing membranes in gap junctions is typically reduced to about 2 nm (57, 58).

Taken together, one can conclude that hDPSC and SCC tumor cells can form gap junctions with one another. This is highly likely as other research groups already indicated gap junction formation between other stem cell types (e.g. bone marrow MSC and adipose tissue derived MSC) and tumor cells (25, 59). Likewise, gap junction formation between tumor cells was already shown (18). The bystander effect therefore might increase since the level of gap junction intercellular communication is predictive for the extent of the bystander effect *in vitro* (60, 61).
However, in this research morphological characteristics were utilized to appoint cells as tumor cells or hDPSC. Although both cell types have a very distinct morphology, cell identification remained subjective. Therefore, to confirm the establishment of gap junctions between hDPSC and tumor cells, it is best to repeat the completed TEM experiment with immune-gold staining directed against a tumor or stem cell marker not expressed by the other cell type. Additionally, the found indicated electron-dense structures were not that common in the cell cultures, probably as a consequence of limited cellular contact between different cells. Elongation of the incubation period of the co-culture could conquer this issue. This is reinforced by Zhurova et al. where cell surface expression of connexin 43 increased with the time of cell culture (62).

4.2 Expression vector design

In order to functionally assess the potency of hDPSC to influence tumor growth through the bystander effect, the suicide gene has to be expressed by the hDPSC. Therefore two expression vectors were

designed. The first expression plasmid was the EF1α-Fluc-HSVtk-MCS plasmid containing the suicide gene HSV-tk, the second plasmid was the EF1α-Fluc-hNIS-MCS or control plasmid.

During the production of the plasmids, restriction analyses indicated the isolation or production of DNA bands with a different restriction pattern and length. These results could be explained by several factors. One aspect is the incomplete dephosphorylation of the vector due to for example enzymatic saturation (63). In such a case, vector closure without the uptake of a phosphorylated insert is more expected during ligation. Inadequate enzymatic restriction, both during the process of vector production and restriction analysis also can explain some results. For example the extra DNA bands in the restriction analysis of the final EF1α-Fluc-HSVtk-MCS plasmid with XbaI. Of course, other possible explanations could elucidate these results such as the use of too few units of enzymes or a too short incubation time although the manufacturer's protocol where followed as strict as possible, etc. (63).

Nonetheless, the final restriction analysis indicated the production of the wanted expression vectors. This was confirmed by sequencing, although one mutation in the HSV-tk gene for all HSV-tk clones was found. The luminescence assay also showed Fluc activity for one EF1α-Fluc-HSVtk-MCS clone. Consequently, for this clone, the functionality of the expression vector is largely demonstrated. The other clones lacked luminescent signal. One possible reason for this could be the limited incubation time for transfection. According to the manufacturer's protocol, cells need to be incubated with the DNA and lipofectamine for one to three days. In our experiment, an incubation period of ±12 hours was applied, possibly resulting insufficient DNA uptake. Repetition of the experiment with an increased incubation time will provide more insight in this matter.

4.3 The 4-nitroquinoline-1-oxide rat model

Novel OSCC treatment is best studied in an animal model strongly resembling its human counterpart. In the current study, oral carcinogenesis was induced by 4NQO administration in rats during nine months. Tissue sections of an eight month long 4NQO-treated rat were used for analysis and optimization. Masson's Trichrome staining demonstrated histopathological changes in the rat tongue. The stratified squamous epithelium displayed features of a pre-malignant dysplastic lesion with ventral outgrowth in the underlying connective tissue in combination with loss of a clear basal membrane. Cell layer specificity and differentiation were also absent at the lesion site.

Immunohistochemistry was performed on the tissue to assess the expression profile of the rat tongue and to be more precise, the keratinized squamous epithelium.

Cytokeratin 19 expression was mainly detected in the oral epithelium dorsal of the basal cell layer. In healthy tongue tissue, cytokeratin 19 is typically expressed in the basal cell layer and functions as a stem cell marker (64). The found increased and suprabasal expression profile of cytokeratin 19 in our results indicate hyperproliferation of the basal cells and has previously been correlated with their premalignant transformation in human tongue samples (65-67), and in 4NQO-treated rats (68).

Connexin 43 positivity was discerned over the entire epithelial cell layer including in the cell mass present in the circumvallate papillae. An increased connexin 43 expression in the 4NQO rat model is in accordance with Feng et al. (68). As indicated previously is connexin 43 expression also present in human OSCC. Overexpression of this protein is related with the presence of tumor cells or the

early stage of tumor promotion (18, 42). The specific contributory role of connexin 43 in OSCC promotion however is not yet known. Nevertheless, evidence indicates an association between connexin 43 expression and the invasive behaviour of OSCC (42, 69). Consequently, connexin 43 may serve as an independent marker for overall survival time (18). In addition, the presence of connexin 43 and the related gap junctions play an important role in stem cell-mediated suicide gene therapy. The passage of the activated prodrug between tumor cells is correlated with the occurrence of gap junction formation and an increased bystander effect.
Finally, malignant transformation of the tongue epithelium was confirmed with the identification of MAGEA3 expression. This accessory protein plays a role in the stimulation of the ligase activity of E3 ubiquitin protein ligases. Furthermore, MAGEA3 stabilizes the E3-E2 conjugating ubiquitin enzyme complex, thereby increasing the ubiquitination and degradation of p53 (70). As a result, manifestation of MAGEA3 is associated with OSCC and an expression increase is associated with tumor dedifferentiation (71).

Taken together, one can confirm that 4NQO administration results in the malignant transformation and tumor development of the tongue epithelium. Other studies already indicated this statement in mice and rats, by 4NQO treatment sessions and by 4NQO addition to the drinking water (72-74). The concentrations in these articles used were higher, explaining the development of large tumor masses and metastasis at a more early time point.

4.4 Overall considerations and future perspectives

Overall, several general considerations need to be taken into account concerning suicide gene therapy and the utilization of stem cells as a gene carrier for future experiments.
One major consideration is the risk of insertional mutagenesis when stem cells are transduced with the suicide gene. Lentiviral transduction of cells can lead to multiple genomic integrations of the transfer DNA. The tendency of the genomic integration is also directed towards actively transcribed genes, entailing a risk of gene disturbance or mutagenesis (75-77). The transactivation of neighbouring genes due to the vector integration can occur as well (78, 79). And although not proven to be detrimental for stem cell-mediated suicide gene therapy, variance in gene expression can arise between stem cells as a result of differences in copy number and integration site (76).
Genome engineering of stem cells with zinc-finger nucleases (ZFN), transcription activator-like effector nucleases (TALEN) or cluster of regularly interspace short palindromic repeats (CRISPR) technologies can be performed to rule out these potential disadvantages. One by one, these genome editing methods ensure targeted integration of a genomic sequence by homologic recombination (80, 81). Insertional mutagenesis is decreased to this end by the selective integration into one specific site of the genome. The AAVS1 locus, an open chromatin structure flanked by insulator elements protecting the integrated transgene(s) from trans-activation or repression, is known to be a safe harbour locus for the integration of transgenes (82). Therefore, specific integration of the suicide gene at this locus through one of these methods would be a safer choice when compared with viral transduction.

Concerning stem cell-mediated suicide gene therapy and the use of stem cells, several other issues need to be taken into account. One is the dosage of stem cells needed to significantly influence tumor

growth. The amount of therapeutic cells necessary to influence tumor growth was already estimated to be less than 10% of the tumor mass (21). Moreover, Kim et al. indicated that repeated injection with a low dose of stem cells exhibits a stronger anti-tumor effect when compared to a single high stem cell dose (83). Further optimization of the dosage and the frequency of administration needs to be accomplished to obtain favourable results. This research project might contribute to dose optimization, since stem cell tracking using BLI is made possible as a result of Fluc expression. The ability to detect the hDPSC *in vivo* in the future makes it possible to implement more accurate dose-response relationship studies.

Specifically for this research, future experiments need to focus on several aspects. First of all, the production of a functional expression vector needs to be confirmed. Consequently, a luminescence assay of the selected expression vectors has to be repeated as previously mentioned. An increased transfection time is recommended. Additionally, the origin of the mutation in the HSV-tk gene can be assessed by sequencing the donated suicide gene vector of Prof. dr. Gambhir. Functionality of the suicide gene and hNIS still needs to be verified too. This can be achieved by assessing the gene expression of HSV-tk and hNIS with immunocytochemistry. Functional evaluation is also a possibility. A hDPSC viability assay can be performed to evaluate HSV-tk expression after GCV addition.
After confirming the production of a complete functional expression vector, the bystander killing effect of hDPSC can be tested. In this context, additional attention has to be addressed towards the use of GCV. To acquire excessive tumor reduction, it is critical to know at which time point and dosage GCV is best administrated. The formation of gap junctions between tumor cells and the therapeutic stem cells being the main determining factor. Consequently, time and dosage experiments need to be conducted first *in vitro*, next *in vivo* to optimize hDPSC-mediated suicide gene therapy. As previously indicated in the discussion, variation in the ratio of hDPSC:SCC might also indicate which amount of stem cells is needed to exert an substantial effect on tumor cell survival. To this extend, co-cultures can be used to evaluate all of these aspects. An Alamar blue assay or a simple trypan blue staining can be executed to examine cell cytotoxicity. Furthermore, increasing the incubation time of the co-culture might result in a more pronounced gap junction formation and is therefore recommended.

In order to optimize the 4NQO rat model, additional immunohistochemistry needs to be implemented. The evaluation of tongue tissue of healthy control rats and other 4NQO-treated rats might give more information about the severity of the cell dysplasia and the most favourable treatment manner to obtain OSCC in rats. Moreover, tumor development over time can be assessed with immunohistochemistry and MRI to have more insight in the tumor progression and location. Currently, *ex vivo* MRI is performed on the head specimen of the animals from the optimization procedure to later correlate the MRI results with the histological data. The MRI parameters are being optimized at this moment.
Additionally, in order to characterise the dysplastic lesions more extensively, expression of additional markers can be tested. For example, presence of ki67, the epidermal growth factor receptor (EGFR) or p53, all markers reoccurring in human OSCC (74, 84). Similar results in our 4NQO rat model will strengthen the choice of this animal model for *in vivo* experiments and increase the relevance of our research even more.

At last, the real-time follow-up of the hDPSC-mediated suicide gene therapy can be conducted in the most favourable 4NQO rat model. The tumor growth or shrinkage after stem cell injection can be monitored with MRI, stem cell viability and location with BLI. Herewith, both observation of the treatment response as therapy guidance are possible. Consequently, the future role of hDPSC in suicide gene therapy can be explored in a similar manner as found in the clinic.

5. CONCLUSION

Over 300,000 people are diagnosed with OSCC each year and the incidence is still rising. Current treatment modalities are associated with severe discomfort and are not able to increase the 5-year survival rate. Therefore, new therapy options need to be explored.

Already numerous studies have been conducted to evaluate the effect of suicide gene therapy on tumor growth *in vitro* and *in vivo*. However, most of these studies rely on the use of viral vector-mediated gene delivery. Although viral vectors assure efficient gene delivery, lack of tumor specificity and safety concerns led to the search of other delivery mechanisms possible to obtain similar or even better results.

By now, several type of stem cells already have been evaluated for their potency as a suicide gene carrier. Despite the many advantages of the hDPSC, no systemic report on the use of hDPSC for suicide gene therapy to treat OSCC is reported, nor for any other type of cancer. Consequently, our research group was the first hypothesizing that hDPSC are a suitable gene carrier in suicide gene therapy for OSCC treatment.

To evaluate the capacity of hDPSC in suicide gene therapy *in vitro*, gap junction formation was evaluated between hDPSC and squamous tumor cells. Immunohistochemical reactivity for connexin 43 and the electron-dense membrane regions at the zones of cell-cell contact indicated gap junctional intercellular communication between hDPSC, tumor cells and both cell types. Based on these data, we propose that hDPSC exert the bystander effect on tumor cells with success. However, the functionality of these gap junctions remain indecisive and demand further attention. Follow-up experiments therefore have to focus on cell viability after hDPSC transduction with a functional expression vector.

Chronic 4NQO administration revealed the formation of a dysplastic lesion of the tongue squamous epithelium in a rat. Whilst several morphological and immunohistochemical parameters verified the malignant epithelial transformation, no metastatic tumor masses in the underlying lamina propria could be found yet. Notwithstanding, the current data imply tumor development after 4NQO exposure. Comparison between the head specimen over time and of different treatment cohorts in the future will give more information about the tumor progression. In addition, real-time evaluation with MRI will define the tumor behaviour in greater detail.

Altogether, the bystander killing effect of hDPSC could not be elucidated yet. Nonetheless, these preceding experiments give a glimpse of the potential of hDPSC in suicide gene therapy. More elaborate research will provide a platform of information about the role of hDPSC for novel therapeutic strategies to treat OSCC or cancer in general.

REFERENCES

1. Jemal A, Bray F, Center MM, Ferlay J, Ward E, Forman D. Global cancer statistics. CA Cancer J Clin. 2011;61(2):69-90.
2. Kanojia D, Vaidya MM. 4-nitroquinoline-1-oxide induced experimental oral carcinogenesis. Oral Oncol. 2006;42(7):655-67.
3. Coelho KR. Challenges of the oral cancer burden in India. J Cancer Epidemiol. 2012;2012:701932.
4. Huber MA, Tantiwongkosi B. Oral and oropharyngeal cancer. Med Clin North Am. 2014;98(6):1299-321.
5. Chi AC, Day TA, Neville BW. Oral cavity and oropharyngeal squamous cell carcinoma-an update. CA Cancer J Clin. 2015;65(5):401-21.
6. Elzahaby IA, Roshdy S, Shahatto F, Hussein O. The adequacy of lymph node harvest in concomitant neck block dissection and submental island flap reconstruction for oral squamous cell carcinoma; a case series from a single Egyptian institution. BMC Oral Health. 2015;15:80.
7. Taibi R, Lleshi A, Barzan L, Fiorica F, Leghissa M, Vaccher E, et al. Head and neck cancer survivors patients and late effects related to oncologic treatment: update of literature. Eur Rev Med Pharmacol Sci. 2014;18(10):1473-81.
8. Ardiani A, Johnson AJ, Ruan H, Sanchez-Bonilla M, Serve K, Black ME. Enzymes to die for: exploiting nucleotide metabolizing enzymes for cancer gene therapy. Curr Gene Ther. 2012;12(2):77-91.
9. Hughes RM. Strategies for cancer gene therapy. J Surg Oncol. 2004;85(1):28-35.
10. Mesnil M, Yamasaki H. Bystander effect in herpes simplex virus-thymidine kinase/ganciclovir cancer gene therapy: role of gap-junctional intercellular communication. Cancer Res. 2000;60(15):3989-99.
11. Pulkkanen KJ, Yla-Herttuala S. Gene therapy for malignant glioma: current clinical status. Mol Ther. 2005;12(4):585-98.
12. Sato T, Neschadim A, Lavie A, Yanagisawa T, Medin JA. The engineered thymidylate kinase (TMPK)/AZT enzyme-prodrug axis offers efficient bystander cell killing for suicide gene therapy of cancer. PLoS One. 2013;8(10):e78711.
13. Moolten FL. Tumor chemosensitivity conferred by inserted herpes thymidine kinase genes: paradigm for a prospective cancer control strategy. Cancer Res. 1986;46(10):5276-81.
14. Greco O, Dachs GU. Gene directed enzyme/prodrug therapy of cancer: historical appraisal and future prospectives. J Cell Physiol. 2001;187(1):22-36.
15. Kim JH, Lee HJ, Song YS. Stem cell based gene therapy in prostate cancer. Biomed Res Int. 2014;2014:549136.
16. Pluta K, Kacprzak MM. Use of HIV as a gene transfer vector. Acta Biochim Pol. 2009;56(4):531-95.
17. Monti M, Perotti C, Del Fante C, Cervio M, Redi CA. Stem cells: sources and therapies. Biol Res. 2012;45(3):207-14.
18. Brockmeyer P, Jung K, Perske C, Schliephake H, Hemmerlein B. Membrane connexin 43 acts as an independent prognostic marker in oral squamous cell carcinoma. Int J Oncol. 2014;45(1):273-81.
19. Wei SJ, Chao Y, Hung YM, Lin WC, Yang DM, Shih YL, et al. S- and G2-phase cell cycle arrests and apoptosis induced by ganciclovir in murine melanoma cells transduced with herpes simplex virus thymidine kinase. Exp Cell Res. 1998;241(1):66-75.
20. Rosolen A, Frascella E, di Francesco C, Todesco A, Petrone M, Mehtali M, et al. In vitro and in vivo antitumor effects of retrovirus-mediated herpes simplex thymidine kinase gene-transfer in human medulloblastoma. Gene Ther. 1998;5(1):113-20.
21. Altanerova V, Cihova M, Babic M, Rychly B, Ondicova K, Mravec B, et al. Human adipose tissue-derived mesenchymal stem cells expressing yeast cytosinedeaminase::uracil phosphoribosyltransferase inhibit intracerebral rat glioblastoma. Int J Cancer. 2012;130(10):2455-63.

22. Kwon SK, Kim SU, Song JJ, Cho CG, Park SW. Selective delivery of a therapeutic gene for treatment of head and neck squamous cell carcinoma using human neural stem cells. Clin Exp Otorhinolaryngol. 2013;6(3):176-83.
23. Leten C, Trekker J, Struys T, Roobrouck VD, Dresselaers T, Vande Velde G, et al. Monitoring the Bystander Killing Effect of Human Multipotent Stem Cells for Treatment of Malignant Brain Tumors. Stem Cells Int. 2016;2016:4095072.
24. Bergfeld SA, DeClerck YA. Bone marrow-derived mesenchymal stem cells and the tumor microenvironment. Cancer Metastasis Rev. 2010;29(2):249-61.
25. Gabashvili AN, Baklaushev VP, Grinenko NF, Levinskii AB, Mel'nikov PA, Cherepanov SA, et al. Functionally Active Gap Junctions between Connexin 43-Positive Mesenchymal Stem Cells and Glioma Cells. Bull Exp Biol Med. 2015;159(1):173-9.
26. Lim TT, Geisen C, Hesse M, Fleischmann BK, Zimmermann K, Pfeifer A. Lentiviral vector mediated thymidine kinase expression in pluripotent stem cells enables removal of tumorigenic cells. PLoS One. 2013;8(7):e70543.
27. Miura M, Gronthos S, Zhao M, Lu B, Fisher LW, Robey PG, et al. SHED: stem cells from human exfoliated deciduous teeth. Proc Natl Acad Sci U S A. 2003;100(10):5807-12.
28. Morsczeck C, Gotz W, Schierholz J, Zeilhofer F, Kuhn U, Mohl C, et al. Isolation of precursor cells (PCs) from human dental follicle of wisdom teeth. Matrix Biol. 2005;24(2):155-65.
29. Seo BM, Miura M, Gronthos S, Bartold PM, Batouli S, Brahim J, et al. Investigation of multipotent postnatal stem cells from human periodontal ligament. Lancet. 2004;364(9429):149-55.
30. Sonoyama W, Liu Y, Yamaza T, Tuan RS, Wang S, Shi S, et al. Characterization of the apical papilla and its residing stem cells from human immature permanent teeth: a pilot study. J Endod. 2008;34(2):166-71.
31. Gronthos S, Mankani M, Brahim J, Robey PG, Shi S. Postnatal human dental pulp stem cells (DPSCs) in vitro and in vivo. Proc Natl Acad Sci U S A. 2000;97(25):13625-30.
32. Huang GT, Gronthos S, Shi S. Mesenchymal stem cells derived from dental tissues vs. those from other sources: their biology and role in regenerative medicine. J Dent Res. 2009;88(9):792-806.
33. Zhao Y, Wang L, Jin Y, Shi S. Fas ligand regulates the immunomodulatory properties of dental pulp stem cells. J Dent Res. 2012;91(10):948-54.
34. Barry FP, Murphy JM, English K, Mahon BP. Immunogenicity of adult mesenchymal stem cells: lessons from the fetal allograft. Stem Cells Dev. 2005;14(3):252-65.
35. Ponnaiyan D, Jegadeesan V. Comparison of phenotype and differentiation marker gene expression profiles in human dental pulp and bone marrow mesenchymal stem cells. Eur J Dent. 2014;8(3):307-13.
36. Perry BC, Zhou D, Wu X, Yang FC, Byers MA, Chu TM, et al. Collection, cryopreservation, and characterization of human dental pulp-derived mesenchymal stem cells for banking and clinical use. Tissue Eng Part C Methods. 2008;14(2):149-56.
37. Wallenius K, Lekholm U. Oral cancer in rats induced by the water-soluble carcinogen 4-nitrochinoline N-oxide. Odontol Revy. 1973;24(1):39-48.
38. Massoud TF, Gambhir SS. Molecular imaging in living subjects: seeing fundamental biological processes in a new light. Genes Dev. 2003;17(5):545-80.
39. Laird DW. Life cycle of connexins in health and disease. Biochem J. 2006;394(Pt 3):527-43.
40. Monteiro BG, Serafim RC, Melo GB, Silva MC, Lizier NF, Maranduba CM, et al. Human immature dental pulp stem cells share key characteristic features with limbal stem cells. Cell Prolif. 2009;42(5):587-94.
41. About I, Proust JP, Raffo S, Mitsiadis TA, Franquin JC. In vivo and in vitro expression of connexin 43 in human teeth. Connect Tissue Res. 2002;43(2-3):232-7.
42. Brockmeyer P, Hemmerlein B, Jung K, Fialka F, Brodmann T, Gruber RM, et al. Connexin subtype expression during oral carcinogenesis: A pilot study in patients with oral squamous cell carcinoma. Mol Clin Oncol. 2016;4(2):298-302.
43. Muramatsu T, Hamano H, Ogami K, Ohta K, Inoue T, Shimono M. Reduction of connexin 43 expression in aged human dental pulp. Int Endod J. 2004;37(12):814-8.

44. Ellis KM, O'Carroll DC, Lewis MD, Rychkov GY, Koblar SA. Neurogenic potential of dental pulp stem cells isolated from murine incisors. Stem Cell Res Ther. 2014;5(1):30.
45. Jiang JX, Gu S. Gap junction- and hemichannel-independent actions of connexins. Biochim Biophys Acta. 2005;1711(2):208-14.
46. Goodenough DA, Paul DL. Beyond the gap: functions of unpaired connexon channels. Nat Rev Mol Cell Biol. 2003;4(4):285-94.
47. Beahm DL, Hall JE. Hemichannel and junctional properties of connexin 50. Biophys J. 2002;82(4):2016-31.
48. Calder BW, Matthew Rhett J, Bainbridge H, Fann SA, Gourdie RG, Yost MJ. Inhibition of connexin 43 hemichannel-mediated ATP release attenuates early inflammation during the foreign body response. Tissue Eng Part A. 2015;21(11-12):1752-62.
49. Martens W, Sanen K, Georgiou M, Struys T, Bronckaers A, Ameloot M, et al. Human dental pulp stem cells can differentiate into Schwann cells and promote and guide neurite outgrowth in an aligned tissue-engineered collagen construct in vitro. Faseb j. 2014;28(4):1634-43.
50. Struys T, Moreels M, Martens W, Donders R, Wolfs E, Lambrichts I. Ultrastructural and immunocytochemical analysis of multilineage differentiated human dental pulp- and umbilical cord-derived mesenchymal stem cells. Cells Tissues Organs. 2011;193(6):366-78.
51. Miko M, Danisovic L, Majidi A, Varga I. Ultrastructural analysis of different human mesenchymal stem cells after in vitro expansion: a technical review. Eur J Histochem. 2015;59(4):2528.
52. Rossignol R, Gilkerson R, Aggeler R, Yamagata K, Remington SJ, Capaldi RA. Energy substrate modulates mitochondrial structure and oxidative capacity in cancer cells. Cancer Res. 2004;64(3):985-93.
53. Youle RJ, van der Bliek AM. Mitochondrial fission, fusion, and stress. Science. 2012;337(6098):1062-5.
54. Leek H, Albertsson M. Electron microscopy of squamous cell carcinoma of the head and neck. Scanning. 2000;22(5):326-31.
55. Tanaka N, Sugihara K, Odajima T, Mimura M, Kimijima Y, Ichinose S. Oral squamous cell carcinoma: electron microscopic and immunohistochemical characteristics. Med Electron Microsc. 2002;35(3):127-38.
56. Kelly DE, Shienvold FL. The desmosome: fine structural studies with freeze-fracture replication and tannic acid staining of sectioned epidermis. Cell Tissue Res. 1976;172(3):309-23.
57. Stevens A, Lowe J. Histologie van de mens. 1ste ed. Houten: Bohn Stafleu Van Loghum; 2007.
58. Bairati A, Gioria M. An ultrastructural study of cell junctions and the cytoskeleton in epithelial cells of the molluscan integument. J Morphol. 2008;269(3):319-31.
59. Matuskova M, Hlubinova K, Pastorakova A, Hunakova L, Altanerova V, Altaner C, et al. HSV-tk expressing mesenchymal stem cells exert bystander effect on human glioblastoma cells. Cancer Lett. 2010;290(1):58-67.
60. Fick J, Barker FG, 2nd, Dazin P, Westphale EM, Beyer EC, Israel MA. The extent of heterocellular communication mediated by gap junctions is predictive of bystander tumor cytotoxicity in vitro. Proc Natl Acad Sci U S A. 1995;92(24):11071-5.
61. Sanson M, Marcaud V, Robin E, Valery C, Sturtz F, Zalc B. Connexin 43-mediated bystander effect in two rat glioma cell models. Cancer Gene Ther. 2002;9(2):149-55.
62. Zhurova M, Woods EJ, Acker JP. Intracellular ice formation in confluent monolayers of human dental stem cells and membrane damage. Cryobiology. 2010;61(1):133-41.
63. BioLabs NE. Troubleshooting Guide for Cloning Ipswich, MA: New England BioLabs; 2016 [Available from: https://www.neb.com/tools-and-resources/troubleshooting-guides/troubleshooting-guide-for-cloning.
64. Abbas O, Richards JE, Yaar R, Mahalingam M. Stem cell markers (cytokeratin 15, cytokeratin 19 and p63) in in situ and invasive cutaneous epithelial lesions. Mod Pathol. 2011;24(1):90-7.

65. Lindberg K, Rheinwald JG. Suprabasal 40 kd keratin (K19) expression as an immunohistologic marker of premalignancy in oral epithelium. Am J Pathol. 1989;134(1):89-98.
66. Ram Prassad VV, Nirmala NR, Kotian MS. Immunohistochemical evaluation of expression of cytokeratin 19 in different histological grades of leukoplakia and oral squamous cell carcinoma. Indian J Dent Res. 2005;16(1):6-11.
67. Zhong LP, Hu JA, Zhao SF, Xu ZF, Ping FY, Chen GF. [Relative quantification of cytokeratin 19 transcription in oral squamous cell carcinoma tissues by fluorescent quantitive real-time RT-PCR]. Zhonghua Kou Qiang Yi Xue Za Zhi. 2006;41(9):553-5.
68. Feng Y, Kang X, Li C, Nie M. [Expression of cytokeratin 19 and connexin 43 in 4-nitroquinoline-l-oxide-induced rat tongue carcinogenesis]. Hua Xi Kou Qiang Yi Xue Za Zhi. 2013;31(3):237-41.
69. Defamie N, Chepied A, Mesnil M. Connexins, gap junctions and tissue invasion. FEBS Lett. 2014;588(8):1331-8.
70. Sun Y. E3 ubiquitin ligases as cancer targets and biomarkers. Neoplasia. 2006;8(8):645-54.
71. Muller-Richter UD, Dowejko A, Peters S, Rauthe S, Reuther T, Gattenlohner S, et al. MAGE-A antigens in patients with primary oral squamous cell carcinoma. Clin Oral Investig. 2010;14(3):291-6.
72. Schoop RA, Noteborn MH, Baatenburg de Jong RJ. A mouse model for oral squamous cell carcinoma. J Mol Histol. 2009;40(3):177-81.
73. Suzuki R, Kohno H, Suzui M, Yoshimi N, Tsuda H, Wakabayashi K, et al. An animal model for the rapid induction of tongue neoplasms in human c-Ha-ras proto-oncogene transgenic rats by 4-nitroquinoline 1-oxide: its potential use for preclinical chemoprevention studies. Carcinogenesis. 2006;27(3):619-30.
74. Minicucci EM, Ribeiro DA, da Silva GN, Pardini MI, Montovani JC, Salvadori DM. The role of the TP53 gene during rat tongue carcinogenesis induced by 4-nitroquinoline 1-oxide. Exp Toxicol Pathol. 2011;63(5):483-9.
75. Ciuffi A. Mechanisms governing lentivirus integration site selection. Curr Gene Ther. 2008;8(6):419-29.
76. Debyser Z. Biosafety of lentiviral vectors. Curr Gene Ther. 2003;3(6):517-25.
77. Wu C, Dunbar CE. Stem cell gene therapy: the risks of insertional mutagenesis and approaches to minimize genotoxicity. Front Med. 2011;5(4):356-71.
78. Pauwels K, Gijsbers R, Toelen J, Schambach A, Willard-Gallo K, Verheust C, et al. State-of-the-art lentiviral vectors for research use: risk assessment and biosafety recommendations. Curr Gene Ther. 2009;9(6):459-74.
79. Hacein-Bey-Abina S, Garrigue A, Wang GP, Soulier J, Lim A, Morillon E, et al. Insertional oncogenesis in 4 patients after retrovirus-mediated gene therapy of SCID-X1. J Clin Invest. 2008;118(9):3132-42.
80. Moore FE, Reyon D, Sander JD, Martinez SA, Blackburn JS, Khayter C, et al. Improved somatic mutagenesis in zebrafish using transcription activator-like effector nucleases (TALENs). PLoS One. 2012;7(5):e37877.
81. Hwang WY, Fu Y, Reyon D, Maeder ML, Kaini P, Sander JD, et al. Heritable and precise zebrafish genome editing using a CRISPR-Cas system. PLoS One. 2013;8(7):e68708.
82. Ogata T, Kozuka T, Kanda T. Identification of an insulator in AAVS1, a preferred region for integration of adeno-associated virus DNA. J Virol. 2003;77(16):9000-7.
83. Kim SW, Kim SJ, Park SH, Yang HG, Kang MC, Choi YW, et al. Complete regression of metastatic renal cell carcinoma by multiple injections of engineered mesenchymal stem cells expressing dodecameric TRAIL and HSV-TK. Clin Cancer Res. 2013;19(2):415-27.
84. Crowe DL, Hacia JG, Hsieh CL, Sinha UK, Rice H. Molecular pathology of head and neck cancer. Histol Histopathol. 2002;17(3):909-14.

SUPPLEMENTARY INFORMATION

Table S1: Oligonucleotide and primer sequences utilized for multiple cloning site construction, suicide gene amplification and expression plasmid sequencing.

Specification	Primer	Sequence	Restriction sites	Company
Production MCS				
MCS1	Forward	5′-CTAGAGTTTAAACGTATACATCGATG TTAACT-3′	5′-PmeI-BstZ17I-	Integrated DNA
	Reverse	5′-CTAGAGTTAACATCGATGTATACGTT TAAACT-3′	CIaI-3′	technologies, Leuven,
MCS2	Forward	5′-GATCCCATATGTTAATTAAGCTAGCG-3′	5′-NheI-3′	Belgium
	Reverse	5′-GATCCGCTAGCTTAATTAACATATGG-3′		
MCS3	Forward	5′-CTAGTGCGATCGCGCCCGGGCATTTA AATCCTGCAGGA-3′	5′-SgfI-SrfI-SwaI-	
	Reverse	5′-CTAGTCCTGCAGGATTTAAATGCCCG GGCGCGATCGCA-3′	SbfI-3′	
Suicide gene amplification				
HSV-tk gene	Forward	5′-CACAGCTAGCATGGCTTCGTACCCCGG CCA-3′	5′-NeI-3′	Integrated DNA
	Reverse	5′-CACAGCGATCGCCGGAATTCCCCGGGTCAG TTA-3′	5′-SgfI-3′	Technologies Leuven, Belgium
Plasmid sequencing				
EF1α-Fluc-HSVtk-MCS plasmid	Forward	5′-GGCCAGCTTGGCACTTGATG-3′	N.A.	Integrated DNA technologies, Leuven, Belgium
	Reverse	5′-GCCCATATCCTTGCCTGATACC-3′		
	Forward	5′-CTGCTTGCGTGAGATTCTCG-3′		
	Reverse	5′-GGACTTCCGTGGCTTCTTGC-3′		
	Forward	5′-CGTGGATTACGTCGCCAGTC-3′		
	Reverse	5′-GCCCGAAACAGGGTAAATAACG-3′		
	Forward	5′-CGGAGGACAGACACATCGAC-3′		
	Reverse	5′-CCTTCTGGGCATCCTTCAGC-3′		
	Forward	5′-GCCCTGTCTTCTTGACGAGC-3′		
Control Plasmid	Forward	5′-GGCCAGCTTGGCACTTGATG-3′	N.A.	
	Reverse	5′-GCCCATATCCTTGCCTGATACC-3′		
	Forward	5′-CTGCTTGCGTGAGATTCTCG-3′		
	Forward	5′-CGTGGATTACGTCGCCAGTC-3′		
	Reverse	5′-CCTTCTGGGCATCCTTCAGC-3′		
	Forward	5′-GCCCTGTCTTCTTGACGAGC-3′		
	Reverse	5′-GGAGCATGAGGGCAAAGACC-3′		
	Reverse	5′-GCGTGGACACGATCAGGAAC-3′		
	Forward	5′-ACGCGGTGTCATGCTTGTG-3′		
	Forward	5′-CTTCATCAAACCTCGGCTGC-3′		
	Reverse	5′- GAATTGGCCGCCCTAGATGC-3′		
	Forward	5′-CTGTGGCATCGTCATGTTTGTG-3′		

Abbreviations: HSV-tk gene: Herpes Simplex Virus type 1 thymidine kinase gene, MCS: Multiple cloning site.

Auteursrechtelijke overeenkomst

Ik/wij verlenen het wereldwijde auteursrecht voor de ingediende eindverhandeling:
Suicide gene therapy for oral squamous cell carcinoma: a stem cell-based approach

Richting: **master in de biomedische wetenschappen-klinische moleculaire wetenschappen**
Jaar: **2016**

in alle mogelijke mediaformaten, - bestaande en in de toekomst te ontwikkelen - , aan de Universiteit Hasselt.

Niet tegenstaand deze toekenning van het auteursrecht aan de Universiteit Hasselt behoud ik als auteur het recht om de eindverhandeling, - in zijn geheel of gedeeltelijk -, vrij te reproduceren, (her)publiceren of distribueren zonder de toelating te moeten verkrijgen van de Universiteit Hasselt.

Ik bevestig dat de eindverhandeling mijn origineel werk is, en dat ik het recht heb om de rechten te verlenen die in deze overeenkomst worden beschreven. Ik verklaar tevens dat de eindverhandeling, naar mijn weten, het auteursrecht van anderen niet overtreedt.

Ik verklaar tevens dat ik voor het materiaal in de eindverhandeling dat beschermd wordt door het auteursrecht, de nodige toelatingen heb verkregen zodat ik deze ook aan de Universiteit Hasselt kan overdragen en dat dit duidelijk in de tekst en inhoud van de eindverhandeling werd genotificeerd.

Universiteit Hasselt zal mij als auteur(s) van de eindverhandeling identificeren en zal geen wijzigingen aanbrengen aan de eindverhandeling, uitgezonderd deze toegelaten door deze overeenkomst.

Voor akkoord,

Erens, Céline

Datum: **8/06/2016**